

Accounts

Carbon Materials and the Surface Modification in View of Electrochemical Li Insertion/Extraction

Tsutomu Takamura

Petoca Materials Ltd., 2-10-1 Toranomon, Minatoku, Tokyo 105-0001

(Received July 25, 2001)

Carbon is an old, and at the same time, a new material. Carbon plays the leading part in the practical design of Li-ion secondary batteries, the most advanced secondary batteries, where as the negative electrode material it takes Li into the internal structure during the charging. This guarantees the reliability and safety by preventing the dangerous deposition of Li metal. In responding to a strong demand of the high power capability, the author has developed several surface modification methods.

This article describes the surface modification methods I have developed, together with several new findings in relation to the behavior of Li in the interior and on the surface of carbon. The following items are described and analyzed: (1) electrochemical reaction rate in relation to the battery reaction could be enhanced by surface modification such as (a) a simple heating in vacuum, (b) mild oxidation, and (c) vacuum deposition of a metal film on the carbon surface with such metals as Ag, Au, Bi, Cu, In, Pb, Pd, Sn, and Zn together with the oxidized ones. The cause of the enhancement was studied on the basis of SEI (solid-electrolyte-interphase); (2) use of a single fiber electrode enabled us to find what really occurs on the electrode surface, to determine the most reliable values of the Li diffusion coefficient in carbon; and to prevent decomposition of propylene carbonate on graphite; (3) electrical contact was demonstrated as a key factor to reduce the initial charging irreversibility and to enhance the cycleability; (4) underpotential deposition of Li on the carbon surface was pointed out; and (5) free movement of Li in metal at an ambient temperature was confirmed by the use of a bipolar cell.

In the final remarks I offer a new term of "carbon alloys" based on the nano-technology, which will be an attractive material both in science and technology in the new century.

Carbon has been attracting human attention as one of the most useful materials since our prehistoric time. Prehistoric peoples painted black colored paintings on the walls of caverns with charcoal formed after firing. Calligraphy has been written with soot-ink that has a long life. Wood charcoal was utilized for a mummy to avoid from its rotting in the tomb. The most recommended electrode materials of fuel cells are carbonaceous materials. And now, fullerenes and nanotubes found in soot are attracting the attention of a large number of scientists and engineers.

Graphite is utilized not only in pencils and nuclear power stations but also in Li-ion secondary batteries as the negative electrode (anode) material. Trends of the battery technology have changed drastically in the last decade of the last century, especially as to the secondary batteries, i.e., a new comer, Li-ion secondary battery, has achieved the top of the production amount among all the secondary batteries in Japan. This is due to the stimulation of new appliances in the IT technology field such as portable telephones, laptop computers, handy cams, etc. All of these portable appliances require high operating voltage, high energy density, and high power density from their power sources. The most promising battery responding to such requirements is Li-ion secondary battery, since its working voltage is as high as over 3 volts, the energy density is over two times that of the other secondary batteries, and it can be compatible for thin handy appliances as thin as less than 5 mm. The remarkable high performances of Li-ion secondary batteries are characterized by utilizing carbonaceous materials as the anode (negative electrode).

Since metallic Li has the most negative standard electrochemical potential (-3.045 V vs H_2/H^+)[1] we can make a high working voltage battery by using Li for the anode, but this has a critical issue when used in the secondary batteries. This is due to the formation of a dendrite or moss structure of Li crystal on the anode surface during the charging process. The crystal is dangerous since it causes firing or explosion due to an internal short during the charging. Such a dangerous phenomenon could have successfully been avoided by the use of carbonaceous materials for the anode active material. Carbonaceous material promote the tendency for Li to be inserted into the interior structure upon negative polarization (battery charging) and to be reversibly released to the electrolyte upon posi-

tive polarization (discharging), whereby it causes no dendrite formation during charging. Natural or artificial graphite is mainly utilized in the commercial batteries in view of high performance and reliability.[2]

In responding to the high power capability it is important to enhance the rate of the electrochemical reaction. Bearing in mind that the electrochemical reaction proceeds at the carbon surface in contact with the electrolyte, we have attempted to enhance the electrochemical reaction of Li insertion/extraction by modifying the carbon surface. In this article the author would like to show how the rate has been enhanced by the surface modification, through which we have found out how fast the Li moves in the carbon structure, and that Li atoms and/or ions move freely even in solid metal at an ambient temperature.

Working Principle of Li-Ion Secondary Batteries

An important feature of Li-ion secondary batteries is that the working principle is based on the mechanism of intercalation of Li in the active materials of the anode and cathode (positive electrode). The schematic figure illustrating the working mechanism is depicted in Fig. 1.[3] At the time of charging, Li^+ in the electrolyte is intercalated into the interior of graphite in the anode, and at the same time, Li intercalated in the interior of $LiCoO_2$ (cathode active material) is deintercalated into the electrolyte from the interior. This mechanism is quite unique in that the amount of electrolyte can be minimized since the reservoir of Li^+ is not the electrolyte but the active materials themselves, which is in contrast to the cases of Ni/Cd and lead-acid batteries.

Because it is similar to absorption phenomenon, which is a physical phenomenon, the intercalation process is so smooth that it gives rise to a high power charge/discharge capability. As stated above, the intercalation prevents the deposition of metallic Li on the anode, which satisfies the safety requirements. The use of a quite restricted amount of the electrolyte allows us to pack a larger amount of the active materials in a restricted volume of the cell container, resulting in an amplified capacity of the cell.

A number of studies have so far been conducted on the insertion of Li in carbonaceous materials in connection with how the electrolyte is in contact with the electrode surface.[4–11] Not only graphite, whether it is natural or artificial, but also mesophase low temperature carbons, hard carbons, and even nanotubes[12] can accommodate Li in their interior structures although the free energy of the accommodation differs depending on the structure.[13–22] The extreme accommodation capacity, i.e., the anode capacity, depends on the carbon structure. The maximum capacity of graphite is determined by referring to the final intercalation formula of C_6Li, which corresponds to 372 mAh/g of carbon. Basically, graphite has a single accommodation site, and Li intercalated in it reveals highly negative and unaltered working voltage until fully discharged although there is a fine structure in the discharging potential caused by the transition of the accommodation stage.[23–26] Different from graphite, low temperature mesophase carbons have at least two different accommodation sites giving rise to two different working voltages on the discharging curve, but the capacity is reported to be as high as over 800 mAh/g.[13–22] Hard carbons have a complicated structure with various sizes of cavities where Li can be accommodated, giving rise to some larger capacity but the discharge potential is not fixed and the discharging rate is slow.[27–29]

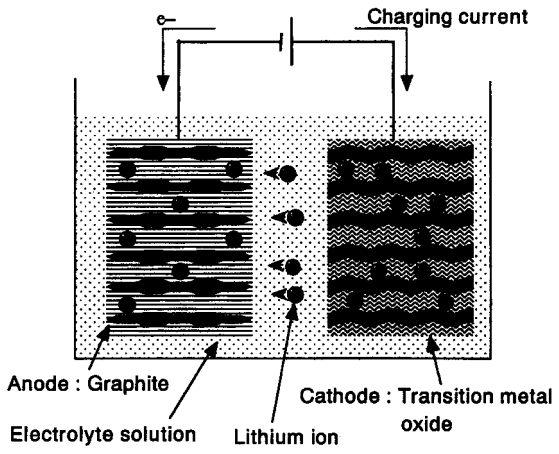

Fig. 1. Schematic model of the working mechanism of Li-ion secondary batteries.

The high Li accommodation amount does not necessarily mean high power discharging ability just like a large volume dam having only a narrow strait gate. The high power charge/discharge ability (high rate capability) is an important key to performance, as well as the high capacity for the secondary batteries. The high rate capability is brought about by the rapid electrochemical reaction rate, and the key factor is the state of the electrode surface. The concept of solid/electrolyte/interphase (SEI) introduced by Peled should be taken into consideration for discussing the reaction rate.[30–33] Any organic substance having oxygen in the molecular structure like the common solvents used in Li-ion batteries is anticipated to be reduced electrochemically at the extreme negative potential near 0 V vs Li/Li^+. This means that the electrolyte is continuously reduced during the charging of the battery. The actual situation, however, reveals no decomposition of the electrolyte provided that the choice of the electrode/electrolyte combination is favorable. This is explained on the basis of the special passivation layer formed on the carbon surface during the first charging process. This special passivation layer is named SEI. The nature of SEI is believed to be dependent on the nature of the carbon surface. In an attempt to provide a high power capability, we have studied how to control the surface of carbon by surface modifications.

Experimental

1 Materials. We selected carbon fibers as the test material since this provides a simple test electrode requiring no binder, no conductive additives, and no coating processes for electrode fabrication. Thus we could avoid the interference of the additives, electrode swelling and deterioration during the electrochemical test. Melblon fibers produced at several heating temperatures (Petoca Materials Ltd. made), were used as an integrated fiber felt or a single fiber. The fiber sample most frequently used was a well-graphitized fiber (Melblon 3100) whose specific surface area is around 1 m^2/g. The SEM images of the fibers with low and high

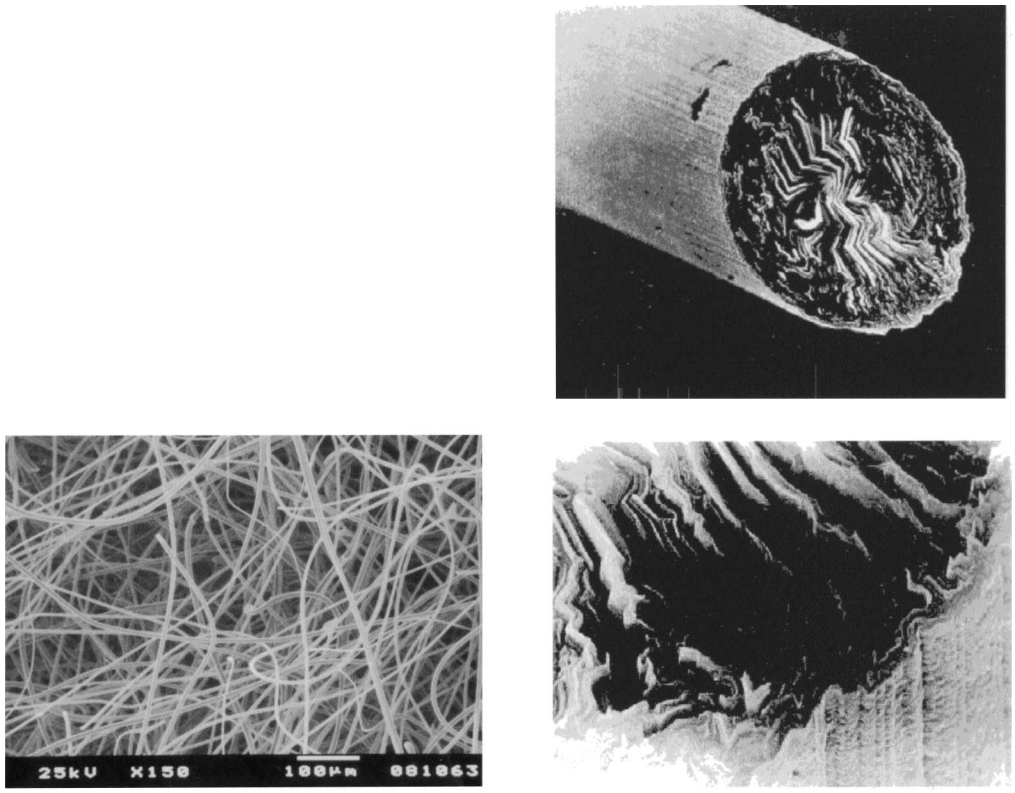

Low magnification

top: medium magnification
bottom: high magnification

Fig. 2. SEM images of highly graphitized MCF carbon fiber (Melblon 3100).

magnifications are shown in Fig. 2. The mean diameter of the fiber was 8.8 µm. In the case of the measurement with a single fiber electrode two types of fibers were examined: a Melblon 3100 fiber and a NF 410–3110 °C fiber which was produced by extruding the fused pitch through a single hole (monofilament technique). The mean diameter of the latter sample was 10 µm. The other mesophase fiber samples examined were those prepared by heating the Melblon felt at 600, 700, 800, 950, 1000, and 1300 °C, respectively. The obtained fibers were heated at 250 °C for 1 h in vacuum and, were used as the standard sample for comparison (later, this is called the pristine sample).

The carbons examined other than the fiber samples were artificial graphite flakes (Timcal), and acetylene black powder, both of these being used without further treatment.

2 Surface Treatment. The simple method performed for the purpose of removing the contaminant adsorbed on the surface was to heat the sample fibers at a desired temperature under a pressure of 10^{-5} Torr for 2 h. This is considered to be effective to remove contaminants such as moisture, oxygen, or surface hydroxy groups adsorbed on the carbon surface.

The second method, which is stronger than a simple heat-treatment, is mild oxidation. The simple way is to heat the sample by covering it with a sufficient amount of acetylene black powder in a crucible at a desired temperature for a definite time. The more rigorous method is to control the partial pressure of oxygen during the heating. This method is effective to remove the contaminants more strongly adhered to the surface, or the passivation layer, by burning them off. The temperature and time of the heat-treatment were varied depending on the nature of the surface. A slight weight loss of the sample was recognized after the mild oxidation.

The third method of the surface modification is the deposition of a metal film on the carbon surface by vacuum evaporation. The sample was mounted in an evaporation chamber and a metal film was deposited by heating a boat containing a pure metal rod at a temperature slightly higher than the melting point of the metal. The thickness of the deposited metal film was controlled by monitoring the weight gain with a vibrating quartz crystal microbalance mounted near the specimen in the vacuum chamber. The metals examined were Ag, Au, Bi, Cu, In, Pb, Pd, Sn, and Zn. The purity of the metals was 99.9% or over.

The fourth treatment is heating the sample covered with a 400 Å thick Ag film in an low pressure atmosphere of oxygen. The temperature and the time were adjusted depending on the effect of the rate enhancement.

3 Fabrication of a Test Electrode. For an integrated fiber felt sample, a 1×1 cm square felt slice with a thickness of 1 mm was sandwiched with a 20 mesh folded Ni expanded sheet of larger size and the rims were spot-welded at several points for tight holding and used as the test electrode. A Ni wire was spot-welded to the expanded sheet prior to sandwiching.

A single fiber electrode was fabricated with a 15 mm long Melblon single fiber or NF single fiber by sticking it on the tip of a rectangular Ni wire with a carbon conductive paste and the Ni wire was fixed to a Teflon made electrode holder. The fiber electrode was placed in a cylindrical Pyrex glass cell vertically.

4 Measurements. Electrochemical measurements were per-

formed with cyclic voltammetry (CV), repeated constant current charge/discharge (CC), and potential step chronoamperometry (PSCA). The electrochemical cell for the felt sample was a three compartment cylindrical Pyrex glass cell (15 mL) where pure Li metallic foils were used as the counter and the reference electrodes. In the case of a single fiber electrode, a two-electrode system was adopted since the resistance overpotential could be ignored due to the very low electrolysis current, less than 40 μA. A rectangular piece of pure Li foil was placed vertically as the counter electrode. CV, CC, and PSCA were conducted with a Hokuto Denko Potentio-galvanostat Model HA-151 joined with a function generator, Model HB-111.

The electrolyte used for the graphitized carbon was a 1:1 (v/v) mixture of ethylene carbonate (EC) and dimethyl carbonate (DMC) containing 1 M of $LiClO_4$. The water contamination level was less than 20 ppm. Pure propylene carbonate (PC) containing 1 M $LiClO_4$ was used for the carbon fibers prepared at low temperature. All the measurements were conducted in a glove box filled with dried argon gas at an ambient temperature.

SEM images were obtained with a JOEL SEM microscope Model 5800 and ^{7}Li NMR measurements were done with a JEOL ECP 300W spectrometer at 117 MHz. Static spectra were obtained at 298 K using a single pulse sequence. 1 M LiCl aqueous solution was used as an external reference for the chemical shift. Ion flame atomic absorption analysis for the Li^+ concentration determination was performed with a Japan Jarrel-Ash Atomic Absorption Spectroanalyzer Model AA-782.

Results and Discussion

1 Graphitized Pristine Sample. The electrochemical reaction occurring at the anode can be simply represented as

$$nC + Li^+ + e^- \underset{\text{discharge}}{\overset{\text{charge}}{\rightleftarrows}} (C_n)Li, \quad (1)$$

where (C_n)Li means that one Li atom is intercalated in n atoms of carbon in the graphite structure. The Li atom intercalated in the graphite interlayer was proved to transfer its electron to graphite to some extent and so it moves in the layer as a positive ion having a partial positive charge.[34]

The cyclic voltammograms (CVs) of a pristine piece of graphitized sample fiber felt with two different potential scan rates are shown in Fig. 3. The reduction current peaks (cathodic peaks) near 0.2 V vs Li/Li^+ are attributed to the electrochemical intercalation of Li into the layers of graphite structure, and the oxidation current peaks (anodic peaks) near 0.3 V are due to the electrochemical deintercalation (extraction) of Li from the graphite structure. The CV obtained with a very slow scan rate gave several well-separated sharp peaks on both the cathodic and the anodic branches. The peak separation can be well interpreted based on the difference in the free energy of stage formation for different stages.[23–26] In case that the electrochemical reaction rates for each stage are fast enough to follow the potential scan rate, a CV having a well-separated fine structure is expected to appear, whereas in the case of the reverse situation, all the peaks will be merged together resulting in one broad peak. Therefore, the degree of peak separation under a constant scan rate is a good measure of the reaction rate. Such will be shown in the case of the surface modification. In regard to cycleability we can easily infer the degree of the cycle life from the degree of degeneration of peak height of

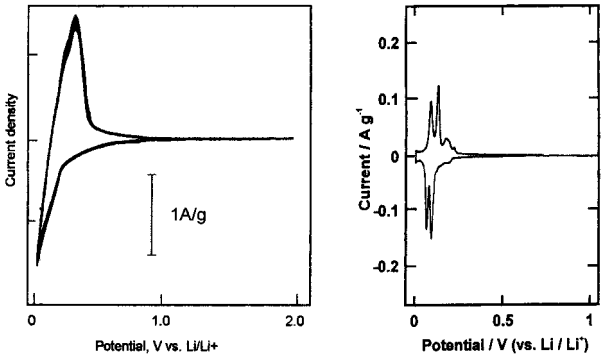

Potential scan rate: (a) 1 mV/s (b) 0.01 mV/s

Fig. 3. CV of well-graphitized carbon fiber felt (Melblon 3100) with a different potential scan rates in EC/DMC containing 1 M $LiClO_4$.[35]

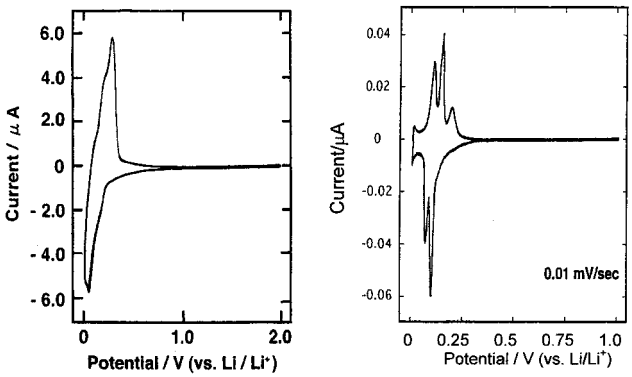

Potential scan rate: (a) 1 mV/s (b) 0.01 mV/s

Fig. 4. CV of a single fiber of well-graphitized carbon (Melblon 3100, ϕ = 8.8 μm) with different potential scan rates in EC/DMC containing 1 M $LiClO_4$[36].

the anodic peak during the repetition of the potential scan.

Figure 4 shows CVs obtained with a tiny single fiber electrode whose surface area is as small as 10^{-3} cm^2. Well-defined CVs that are very similar to those obtained with an integrated fiber felt could be obtained, indicating that the study with a single fiber electrode is reliable.[36]

Reversible expansion and shrinkage of a graphitized fiber during the Li insertion/extraction were first observed under a microscope by Uratani.[37]

In contrast to the well-graphitized carbon, a low graphitization carbonaceous material formed at low temperature gave a CV pattern different from that of the graphitized one, this is shown in Fig. 5. Two broader peaks were revealed on both the cathodic and the anodic branches, which could not be split into a fine structure even with the slowest scan rate (Fig. 5 (B)).[38] Features of the Li accommodation in the low temperature carbon will be discussed later in terms of the loose distribution of the internal fine structure.

The XRD patterns of a mesophase well-graphitized carbon fiber (Melblon 3100) and a mesophase low graphitization carbon fiber are compared in Fig. 6.[38] The former shows two sharp peaks at around 27 and 56° that are due to graphite struc-

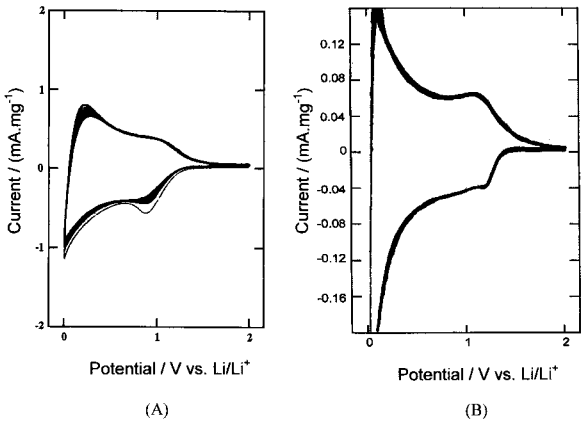

Fig. 5. CV of a disordered mesophase carbon fiber felt prepared at 800 °C (Melblon 800) obtained in PC containing 1 M $LiClO_4$ with two different potential scan rates of 1 mV/s (A), and 0.02 mV/s (B).[38]

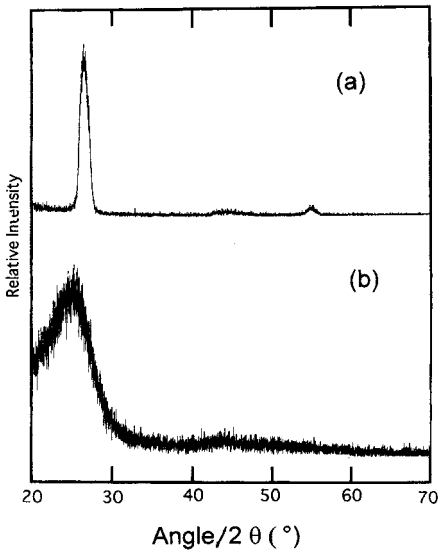

Fig. 6. XRD of a mesophase well-graphitized carbon fiber prepared at 3100 °C (a) and a mesophase low graphitization fiber prepared at 800 °C (b).[38]

ture comprised of graphene layers with parallel orientation, whereas the pattern of the latter indicates that the solid is not well crystallized but has tiny crystallites whose structures are graphite-like.

2 Effect of Heat-Treatment in Vacuum.[39–42] A simple evaluation of the cycleability of the test material is to measure the depression ratio of the peak height of the anodic peak during a definite repetition of the charge/discharge based on the initial peak height. For example, the anodic peak height of the CV in Fig. 3 (a) decreases 10% within 20 repetitions of the charge/discharge cycles, while the peak height decrease of the 1000 °C- prepared carbon (Fig. 7 (a)) within the same cycles is 21%, showing that the cycleability of highly graphitized fiber is far better than that of a low temperature carbon fiber. In addition to the simple cycle behavior the initial charging behavior differs also between the two carbons, which can be recognized by comparing the two CV curves.

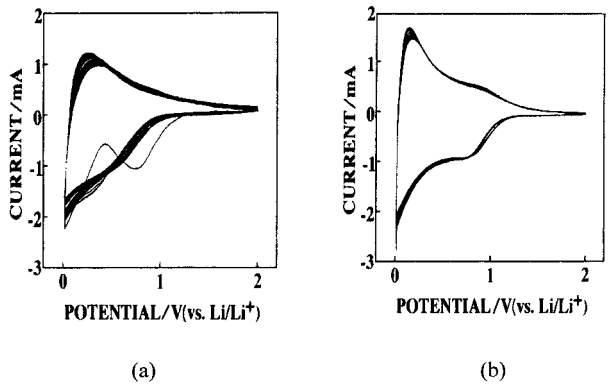

Fig. 7. CVs (in PC containing 1 M of $LiClO_4$) of a disordered mesophase carbon prepared at 1000 °C before (a) and after (b) the heat-treatment in vacuum.[39]

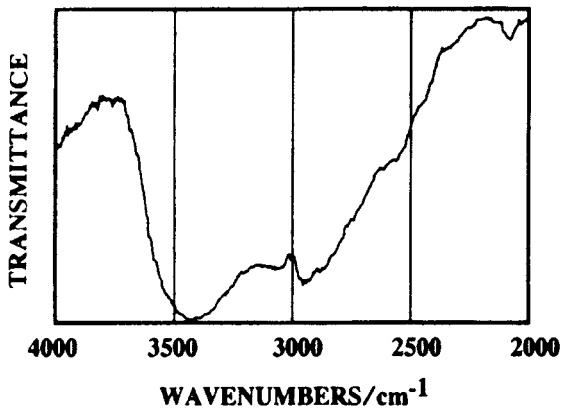

Fig. 8. FTIR difference spectrum of a mesophase carbon fiber felt prepared at 1000 °C. The spectrum was obtained by subtracting the spectrum of the heat-treated (950 °C) fiber felt from that of a non-treated one.[39]

We examined the effect of heat-treatment. The 1000 °C pristine sample was heat-treated at 950 °C for 1 h under the vacuum pressure of 10^{-5} Torr. The resulting CV curve was quite much improved both in cycleability and the initial charging behavior, as shown in Fig. 7 (b). The cause of the improvement was examined on the basis of the surface contaminant. Since the heat-treatment temperature is 50 °C lower than that of the preparation temperature, a change in the internal structure is unlikely during the heat-treatment. The noticeable change in the CV profile could be attributed to the removal of the surface hydroxy groups by the heat-treatment.

The presence of the surface hydroxy group could be detected by FTIR. The FTIR difference spectrum shown in Fig. 8 was obtained by subtracting the FTIR transmittance spectrum of the heat-treated sample from that of the pristine one. A strong broad absorption band appearing at about 3400 cm^{-1} in the difference spectrum is reasonably assigned to the ν_{OH} of surface –OH groups which had been removed by the heat-treatment. The presumption that the –OH group was on the surface and not in the carbon interior could be verified by the following results. The heat-treated sample exposed to the anodic oxidation in an aqueous sulfuric acid solution gave rise to the presence of a large amount of –OH in FTIR, the corre-

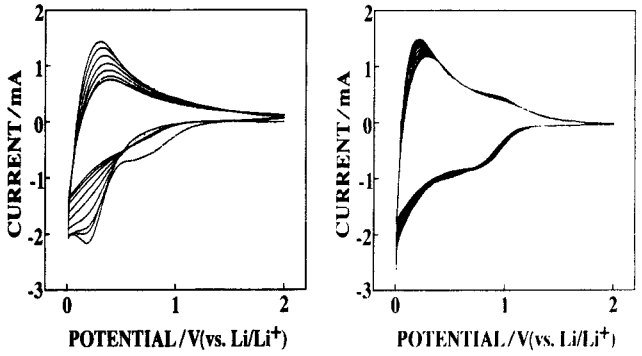

(a) (b)

Fig. 9. CVs (in PC containing 1 M of $LiClO_4$) of a disordered mesophase carbon prepared at 1000 °C before (a) and after (b) the heat-treatment at 600 °C for 5 min. Sample (a) was obtained by anodizing the sample (b) in Fig. 6 in an aqueous H_2SO_4.[39]

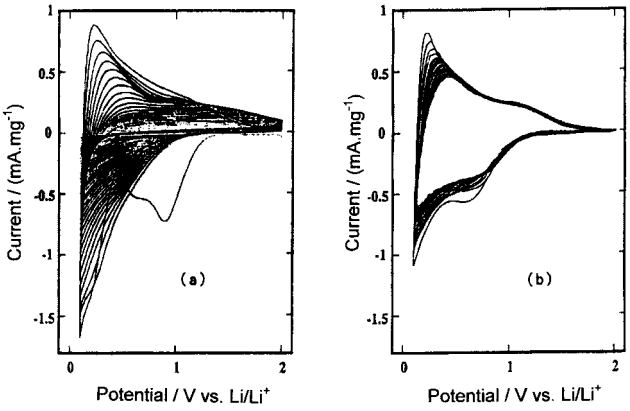

Fig. 10. CVs of a disordered mesophase carbon fiber fired at 700 °C (Melblon 700) in PC containing 1 M $LiClO_4$ before (a) and after (b) the mild oxidation treatment. Potential scan rate: 1 mV/s.[41]

sponding CV being shown in Fig. 9 (a), but the profile of the CV was converted into one very similar to Fig. 7 (b) after the heat-treatment at 950 °C, the profile being shown in Fig. 9 (b).[39]

3 Mild Oxidation.[40–42] The effect of mild oxidation is to remove the surface contaminant or surface retarding layer just like burning it off. Practically, the sample is heated under a low-pressure oxygen atmosphere for a definite time. The treatment conditions including temperature, pressure of oxygen, and treating time should be adjusted to obtain a good result. Different from the heat-treatment in vacuum, the mild oxidation temperature is low enough to avoid any structural change of the carbon sample. We tried to apply mild oxidation to the low temperature carbons by heating the sample covered with a sufficient amount of acetylene-black powder in a crucible. When examined with the same sample as described in Section 2 we could obtain very similar results at 600 °C for 5 min. The effect of mild oxidation was demonstrated with a much disordered carbon having a very poor cycleability. The results are shown in Fig. 10,[41] where we can recognize that not only the initial irreversible charging but also the cycleability are improved to a great extent. The Li insertion/removal performance was greatly enhanced for a well-graphitized fiber as well (Fig. 11). The rate enhancement can be inferred from an increased peak height, sharpened shape of the peak, and a shift of peak position to the negative potential side.[41] Surface roughening due to mild oxidation can be recognized by comparison of the SEM images before and after the treatment (Fig. 12).

Mild oxidation was also found effective to enlarge the double layer capacity of active carbons. Electrical double layer has been utilized for forming a capacitor whose capacity is as huge as millions times of the conventional electrolytic capacitor. The working principle of the capacitor is utilizing the double layer capacity of a material having a very large specific surface layer. Active carbons are promising candidates as electrode material. The very high specific surface area of active carbon is due to the presence of millions of tiny tortuous micro-pores on the surface. Since the openings of the micro-

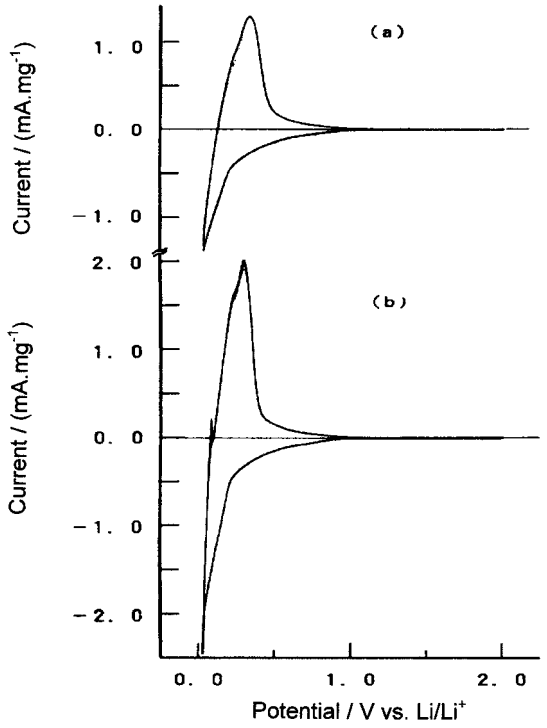

Fig. 11. CVs of a well-graphitized carbon fiber felt (Melblon 3100) in EC/DMC containing 1 M $LiClO_4$ before (a) and after (b) the mild oxidation treatment in air. Scan rate: 1 mV/s.

pores are bottleneck like and the diameters are almost as small as nanometers, entrance of ions into the pores is prevented resulting in giving only a part of the expected large capacity, i.e., less than half than that of the expected capacity.

We attempted to enlarge the openings by mild oxidation for increasing the capacity. An example is shown in Fig. 13 for Kuractive #2500 (Kuraray Chemicals, Co.) whose specific surface area determined by nitrogen adsorption is estimated to be 2500 m^2/g and whose ideal capacity is expected to be over 400 F/g. The CV obtained with the pristine active carbon fiber is shown in Fig. 13 (a), which reveals typical shape for a capaci-

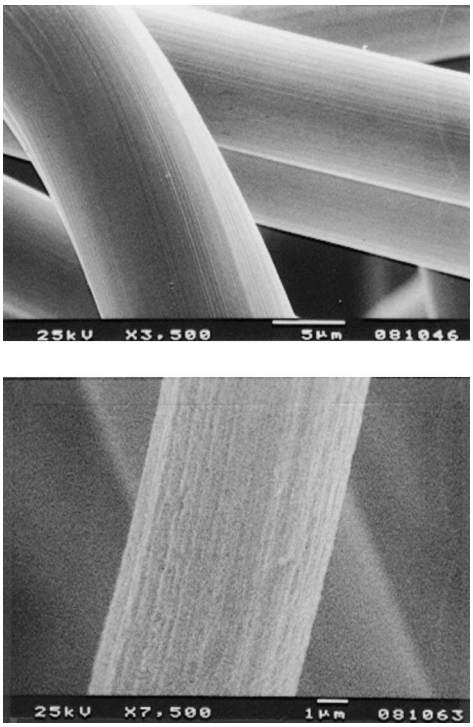

Fig. 12. SEM images of a well-graphitized carbon fiber (Melblon 3100) before (top) after (bottom) the mild oxidation treatment in air.

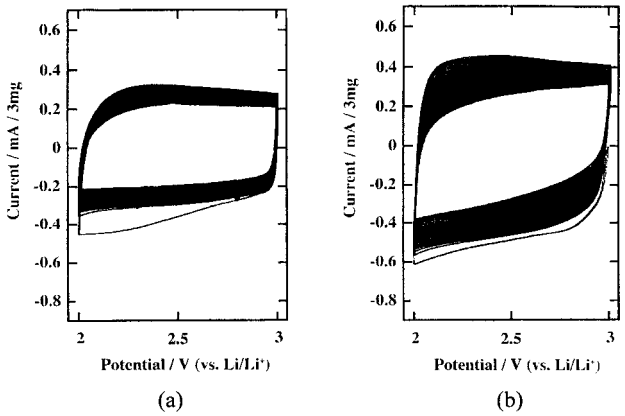

Fig. 13. CVs of an active carbon textile (Kuractive # 2500) in PC containing 1 M $LiClO_4$ before (a) and after (b) the mild oxidation treatment at 600 °C for 5 min.[42]

tor though the capacity decreased progressively with the repetition of charge/discharge cycles. The actual capacity obtained was 100 F/g that is only one fourths of the theoretically expected one. After the mild oxidation treatment at 600 °C for 5 min, the obtained CV was enlarged to about 1.5 times as that of original as shown in (Fig. 13 (b)).[42] The capacity determined with the first cycle curve was 150 F/g indicating the effectiveness of mild oxidation. The issue to be solved is how to minimize the degeneration during the cycles.

4 Metal Film Deposition by Vacuum Evaporation. If the diffusion rate of Li in the interior of graphite is sufficiently rapid we can increase the Li charging/discharging rate by mod-

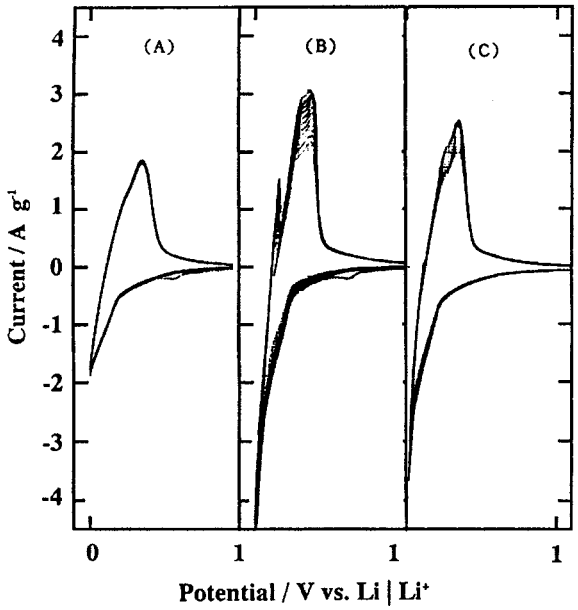

Fig. 14. CV of well-graphitized carbon fiber in EC/DMC containing 1 M $LiClO_4$ without (A) and with an evaporated Pd film. Thickness: (B) 150 Å; (C) 500 Å.[44]

ifying the carbon surface as shown in the preceding sections. We have provided a novel method of the surface modification with a simple vacuum evaporation. We could show that Li can be inserted in and removed from carbon through a Pd film deposited in vacuum.[43] Two years later we could succeed in showing the peak enhancement effect by a Pd-deposited film though the cycleability was unfavorable (Fig. 14).[44] Deposition of a Au film on a well-graphitized carbon fiber felt showed gold color when the thickness was over 200 Å and the resulting CV revealed a peak height increasing as shown in Fig. 15.[44] Such peak height enhancement can be recognized by comparing with that of bare carbon shown in Fig. 14 (A). The gold film was found to cover all over the carbon surface as shown in Fig. 16. Here a part of the top is shown to be removed by scratching by which we could recognize that the Au film covers the entire surface of the carbon fiber uniformly; otherwise we could not differentiate the surface from that of carbon. Even though the film is as thin as 150 Å, the whole surface involving the cross section appears to be covered with a Au film compactly, implying that a thicker film will provide a more perfect covering.

A remarkable enhancing effect was found with a 400 Å thick Ag film whose feature is compared with that of bare carbon in Fig. 17.[35,44,45] Not only the rate enhancement but also a good cycleability was provided by the Ag film deposition. A SEM image of the Ag-covered carbon fiber is shown in Fig. 18,[46] where we can see that a part of the deposited Ag film at the top was removed by scratching. Different from the case with Honbo and co-workers,[47] this allows us to assume that the electrochemical reactions take place on the surface of the Ag film in contact with the electrolyte solution and that the Li atom formed by the reduction reaction is taken into the metallic Ag and moves through the film to the Ag/C interface, then jumps across the interface into the carbon interior, and vice versa. One may assume that the Ag film was not compact but

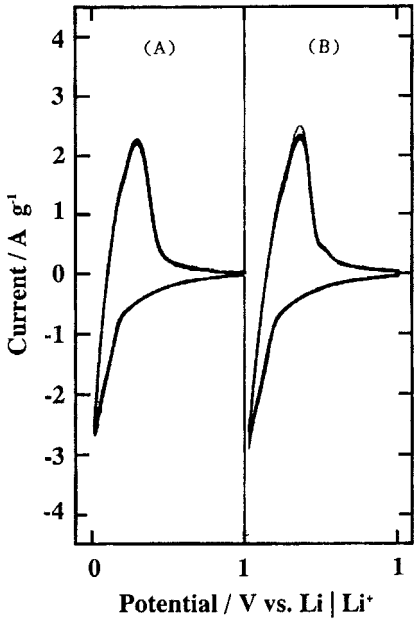

Fig. 15. CV of a well-graphitized carbon fiber felt in EC/DMC containing 1 M $LiClO_4$ with an evaporated Au film. Thickness: (A) 150 Å; (B) 300 Å.[44]

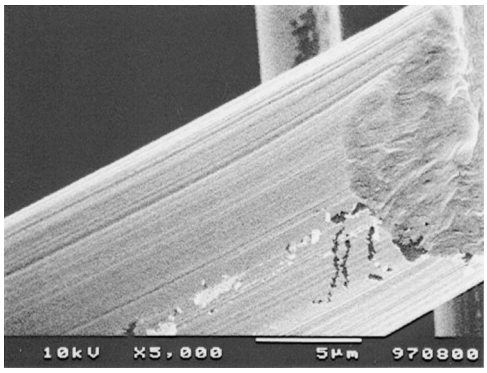

Fig. 16. SEM image of a 150 Å thick Au film vacuum deposited on a well-graphitized carbon fiber. Small front parts were scratched to remove the film for confirming the presence of the covering film.

was sufficiently porous that the direct reaction on the bare carbon surface in contact with the electrolyte could easily occur, but in this case the rate is supposed to be much reduced due to the restricted bare surface area. The stability of the Ag film deposited on the carbon surface was verified by taking XRD patterns of the metal covered carbon fiber before and after the measurement of 20 times CV cycles in EC/DMC containing 1 M $LiClO_4$, the results being shown in Fig. 19.[35]

The rate enhancement due to the presence of the vacuum deposited film can be elucidated by assuming that the electrochemical reactions are facilitated on the surface of metal film as compared with the case on the bare carbon surface of the pristine sample. As is easily inferred by comparing Figs. 14 to 16, the degree of the rate enhancement effect was found to depend on the nature of the metal, which will be explained in detail later by taking the nature of SEI into consideration.

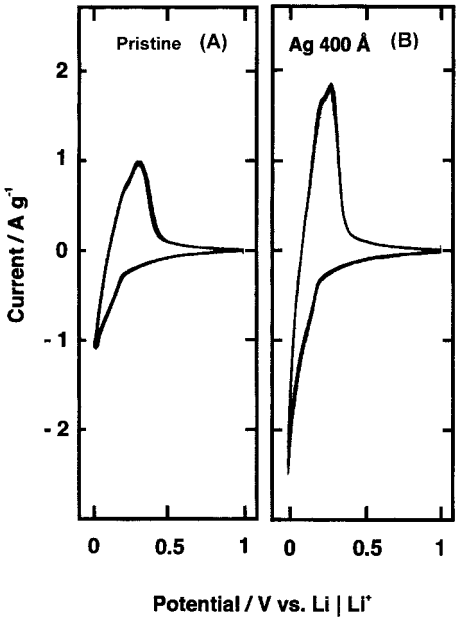

Fig. 17. CVs of without (A) and with (B) a 400 Å thick Ag film in EC/DMC containing 1 M $LiClO_4$.

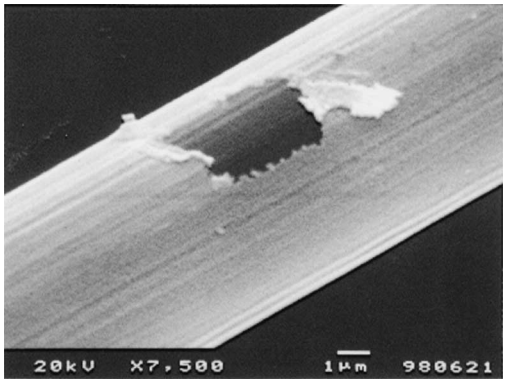

Fig. 18. SEM image of a well-graphitized carbon fiber covered with a 300 Å thick Ag film whose top part was scratched to remove the film.[46]

The enhancing effect of a Ag film somewhat complicatedly depended on the film thickness, as shown in Fig. 20.[35] Such a complicated behavior, which is in contrast to a simple behavior of Cu, can be attributed to the fact that the orientation of each Ag crystal face varies depending on the thickness. The electrochemical reaction rate is supposed to depend on the crystal face in contact with the electrolyte. The CVs obtained with fibers loaded with deposited films of Zn and Pb are shown in Figs. 21 and 22.[44,47] Both metals revealed the peak enhancing effect while the cycleability differed very much. Zn gave a very stable peak during 20 cycles in contrast to the case of Pb that revealed progressive degeneration of the peak height. The major difference between the two cases is related to the cause of the stability of the additional anode peaks appearing in the positive side region from the main Li deintercalation peak. These side peaks are attributed to the anodic removal of Li from the Li alloys formed with the metals during the reduction process. Formation of Li alloys was ascertained by the XRD

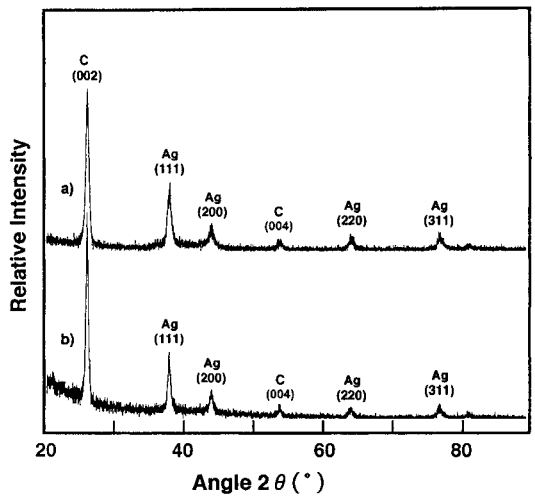

Fig. 19. XRD patterns of a carbon fiber (Melblon 3100) loaded with a Ag film before (a) and after (b) the 20 times of CV cycles. Film thickness: 400 Å.[35]

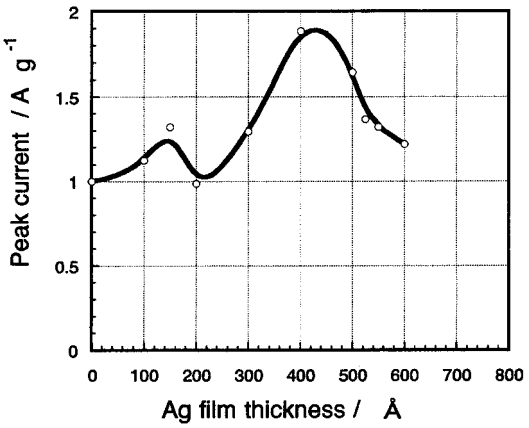

Fig. 20. Film thickness dependency of the relative height of CV peak for Li inter-/deintercalation on Melblon 3100 in EC/DMC electrolyte.[35]

patterns obtained with the metal film deposited on a Ni plate. Stability of the Li alloys during the insertion/removal cycles was different from metal to metal, and the film thickness influenced the result as well. CVs obtained with a Pb film vacuum-evaporated on a Ni plate revealed that the peak heights of all the peaks were reduced rapidly during the cycles.[47] This is attributed to the collapse of the deposited Pb film during the insertion/removal cycles, which might be caused by a large expansion/shrinkage.

5 Rate of Alloy Formation Revealed on CV.[35] Many metals form alloys with Li with a variety of composition ratios. The rates of the alloy formation and decomposition differ depending on the stability and the crystal size of each alloy. We found that the profile of CV peaks due to the alloy formation and decomposition was strongly dependent on the potential scan rate in the case of Ag film deposited on a Ni plate. A 400 Å thick Ag film was vacuum-deposited on a Ni plate and the CV was recorded in EC/DMC containing 1 M $LiClO_4$ with different potential scan rates. Typical examples are shown in

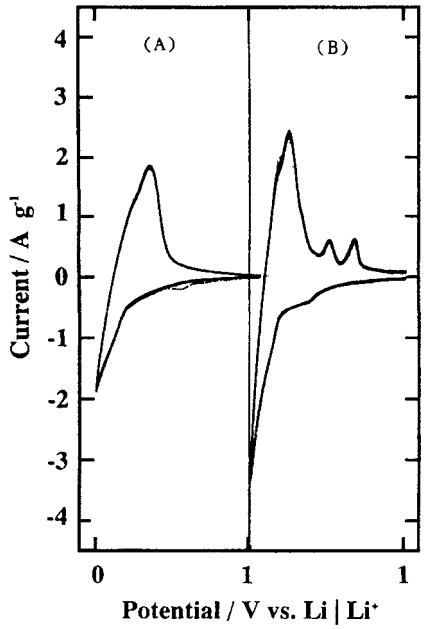

Fig. 21. CVs of a well-graphitized carbon fiber (Melblon 3100 in EC/DMC containing 1 M $LiClO_4$) without (A) and with (B) a 300 Å thick Zn film vacuum deposited. Scan rate: 1 mV/s.[44]

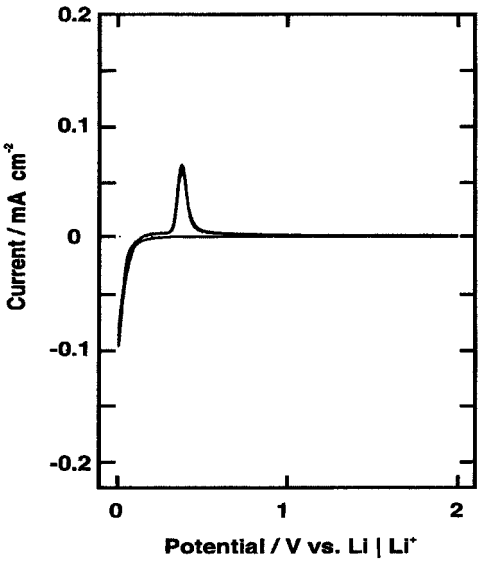

Fig. 22. CV of a 400 Å thick Ag film deposited on a Ni plate measured in EC/DMC containing 1 M $LiClO_4$ with a potential scan rate of 1 mV/s.[35]

Figs. 22 and 23. The CVs were quite different from each other: the one obtained with a faster scan rate gave only a single peak on both the reduction and the oxidation scanning curves, while the latter gave several sharp peaks.[35] However, a peak at about 0.3 V on the anode scan curves is common to both cases, implying that the rates of formation and decomposition of the corresponding alloy are fast enough to follow the scan rate. It is interesting to note that, in spite of such a complicated nature of the Ag film, the stability of the crystal structure of the film is quite high as shown in Fig. 19.[35]

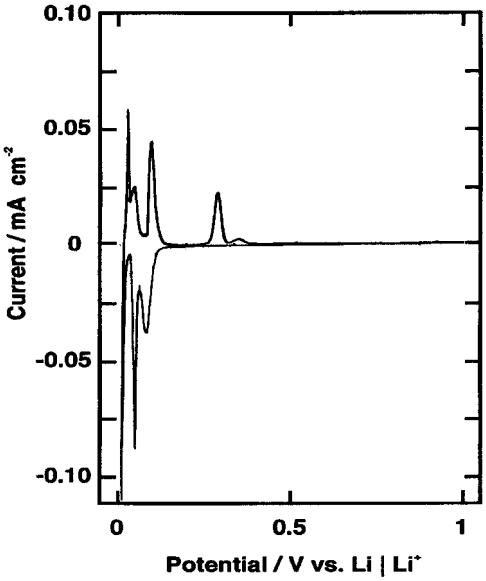

Fig. 23. CV of a 400 Å thick Ag film deposited on a Ni plate measured in EC/DMC containing 1 M $LiClO_4$ with a potential scan rate of 0.01 mV/s.[35]

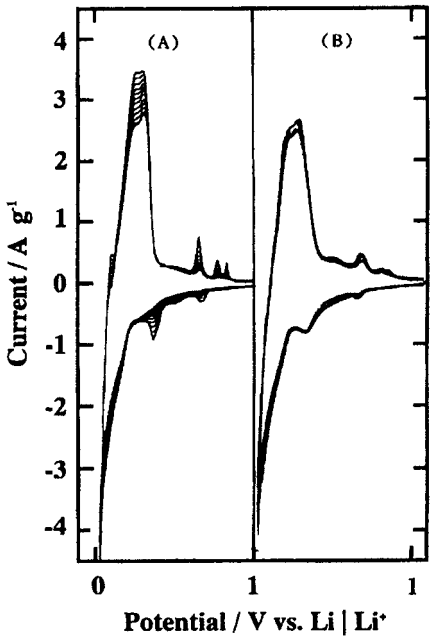

Fig. 24. CVs of a well-graphitized carbon fiber (Melblon 3100) felt covered with a 300 Å thick Sn film before (A) and after (B) the mild oxidation treatment. In EC/DMC containing 1 M $LiClO_4$. Scan rate: 1 mV/s.[48]

The reason why the potentials of the insertion and the removal of Li in a Ag film do not coincide with each other independent of the scan rate is not clear and will be given attention by many researchers, but this will be put aside here since such analysis is beyond the scope of this article.

6 Improvement of Reversibility by Oxidizing the Deposited Metal Film. Some metal films deposited on carbon fiber were found to give poor cycleability. In Fig. 24 an example of Sn film is shown.[44,48] As seen in Fig. 24 (A) the peak

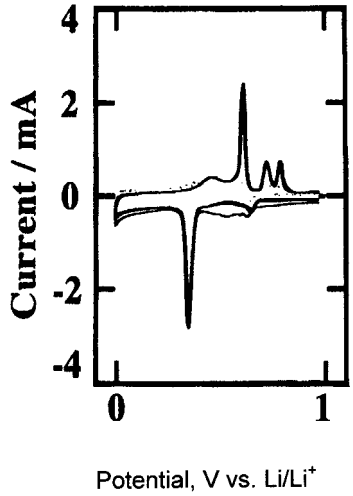

Fig. 25. CV of a 300 Å thick Sn film deposited on a Ni plate, measured in EC/DMC containing 1 M $LiClO_4$. Scan rate: 1 mV/s.

height due to the extraction of Li intercalated in the graphitized carbon was depressed progressively during the repetition of cycles, despite the peak height enhancement. The spike-like peaks are attributed to the insertion and extraction of Li into and out of Sn film, which can be easily inferred when we refer to the CV obtained with a Sn film deposited on a Ni plate (Fig. 25). The presence of a crystallized Sn film can be confirmed by referring to curve (A) in Fig. 24. The progressive depression of the peak height was ascribed to the collapse of the metallic Sn film due to the large expansion/shrinkage during the repetition of CV cycles. The crystal collapse will cause a complicated loose structure of SEI to form, which is not favorable for keeping good cycleability.

We examined the effect of oxidized Sn film, since Idota and co-workers reported that an amorphous form of tin oxide revealed a good anode cycleability while keeping an extraordinary high capacity.[49] The CV results obtained after the oxidation are shown in Fig. 24 (B), where we see the cycleability is improved quite well not only for carbon but also for Sn. The carbon surface was still covered with the film even after the oxidation, as can be inferred from a SEM image shown in Fig. 26. The XRD patterns in Fig. 27 show that the Sn crystal formed by the vacuum evaporation (curve A) changed to some oxides (curve B) after mild oxidation, but these disappeared after the CV cycles (curve C). A clearer situation will be recognized if we see several sub-peaks of Fig. 24 (A) due to Li–Sn alloys. The peak position is identical with that observed with a metallic Sn Fig. 25 but the peak width after the oxidation treatment is broadened implying the formation of a loose structure similar to amorphous one. Becoming amorphous is expected to prevent the collapse of the crystal, because in this structure the expansion and shrinkage during the CV cycles is supposed to be minimized. Such an effect could also be seen for the case of In.[44] The cycleability was quite improved after the oxidation where we see a large initial irreversible charging curve at around 0.8 V. This can be attributed to the reduction of indium oxides formed by the oxidation. A similar tendency was found for Bi as well.[50] Now we can provide a simple way to realize

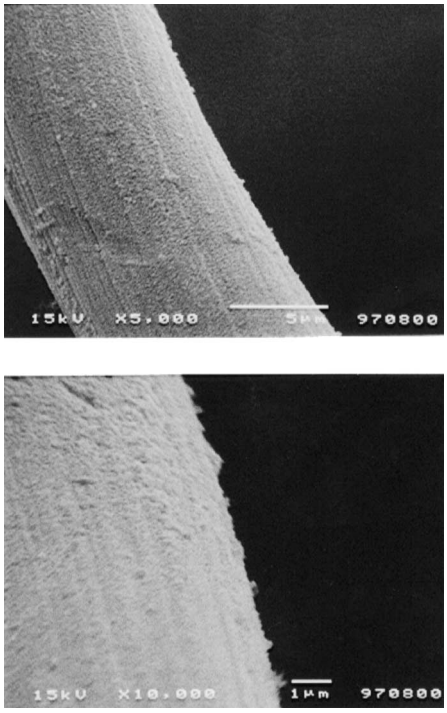

Fig. 26. SEM images of a well-graphitized carbon fiber (Melblon 3200) covered with a 300 Å thick Sn film before (top) and after (bottom) mild oxidation.[48]

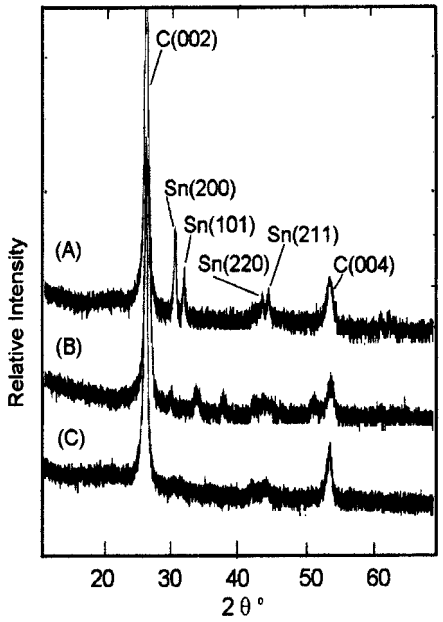

Fig. 27. XRD patterns of a well-graphitized carbon fiber (Melblon 3100) covered with a 300 Å thick Sn film. (A) before the CV measurement; (B) after the mild oxidation treatment; (C) measured with (B) after exposing to the CV cycles.[48]

the structural change from crystal to amorphous, i.e., the film is exposed to oxidation followed by the electrochemical reduction, by which the cycleability improvement is attained.

7 Cause of the Performance Improvement by Metal Film Deposition.

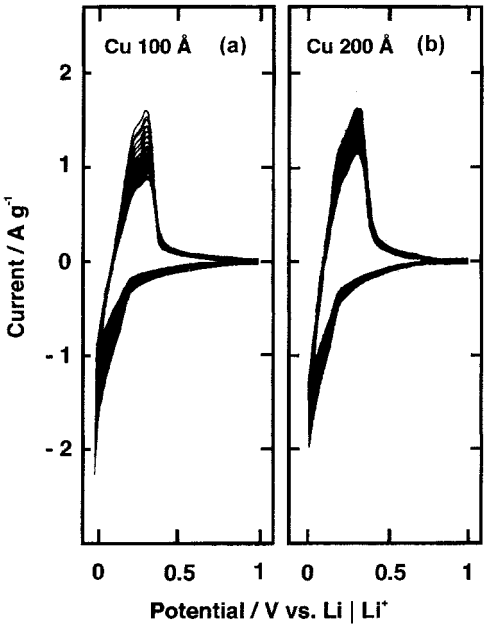

Fig. 28. CVs of a well-graphitized carbon fiber (Melblon 3100) covered with a Cu film for two different thicknesses. In EC/DMC containing 1 M $LiClO_4$. Scan rate: 1 mV/s.

We would like to discuss the electrochemical performance in terms of SEI. The chemistry of SEI is not clear even with a number of studies on SEI so far carried out that were mainly based on methods of sophisticated analytical chemistry.[31–33] The proposed structure is too complicated to identify where is the electrochemical reaction site controlling the Li insertion/extraction reactions is. This means that the chemical entities detected even with sophisticated instruments on the carbon surface cannot necessary be attributed to the substances in question that are really controlling the electrochemical reaction. Bearing in mind this issue we preferred to utilize an indirect method for identifying the cause of the performance improvement that, however, is expected to give results more reliable for the present purpose.

The novel method proposed by us is to deposit further a different metal film over the surface of an already covered metal, whereby each obtained CV result can be examined carefully. A good example is a combination of Cu and Ag. When we deposit a Cu film on the bare surface of a well-graphitized carbon fiber we obtain a CV profile like those shown in Fig. 28. Comparison of these CVs with that of pristine fiber shown in Fig. 3 (a) indicates the Cu film impairs the cycleability, which is in contrast to the case of Ag film shown in Fig. 29 (left). Good cycleability obtained with a Ag film, however, turned worse when we deposit a Cu film over the surface of Ag film, which is shown in Fig. 29 (right). Possible causes of the cycleability deterioration are: poor contact of Cu film with the substrate, porous structure of the deposited Cu film, and the formation of an unfavorable SEI on the Cu surface. The first postulate can be examined by depositing a Ag film over the surface of Cu that covers the substrate carbon.

The results are shown in Fig. 30, which clearly shows that the poor cycleability of a Cu covered fiber was improved remarkably. This result verifies that the electrical contact of Cu

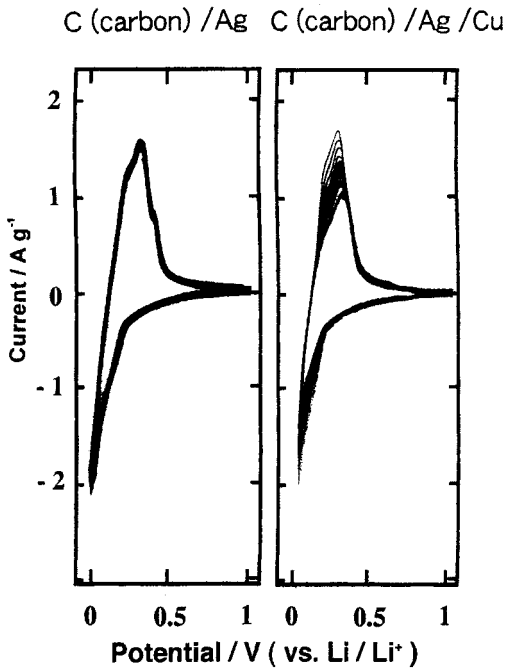

Fig. 29. CVs of a well-graphitized carbon fiber (Melblon 3100) covered with a 400 Å thick Ag film (left) and that covered with a 400 Å thick double layer film consisting of 200 Å thick Ag inner layer and 200 Å thick Cu outer layer.

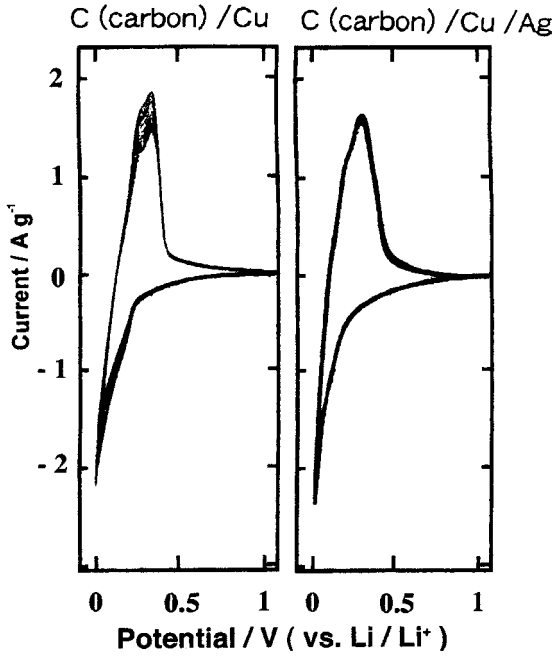

Fig. 30. CVs in EC/DMC containing 1 M $LiClO_4$ for a well-graphitized carbon fiber (Melblon 3100) covered with a vacuum deposited 600 Å thick Cu film (left) and a double layered film (right), whose inner layer is 300 Å thick Cu and whose outer is 300 Å thick Ag. Scan rate: 1 mV/s.

with carbon was not poor. A fiber covered with a two ply-layer metal film of Ag/Cu shown in Fig. 29 (right) revealed a poor cycleability, while it changed to reveal a very stable cycleability when covered further with an over-layer of a Ag film, which is shown in Fig. 31. The fact that in spite of the most complicated layer structure a very stable cycleability was obtained with a fiber covered with a triple layered film where the outer layer is Ag indicates that the most important factor for obtaining a good cycleability is to cover with a Ag film as the outermost layer. Whenever a Cu layer covers as the outermost layer the cycleability is poor irrespective of the layer structure. Therefore, we can conclude that an SEI formed on a Ag film is a favorable one for reversible Li insertion/removal reaction while that on a Cu film is unfavorable. The reason why an SEI formed on a Cu layer is unfavorable remains to be studied further.

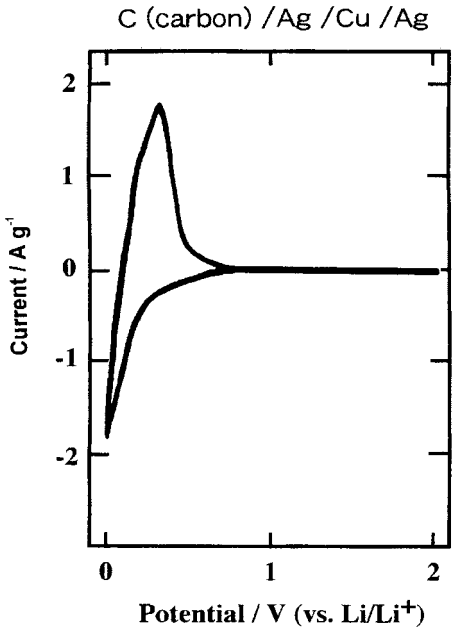

Fig. 31. CVs in EC/DMC containing 1 M $LiClO_4$ for a well-graphitized carbon fiber (Melblon 3100) covered with a vacuum deposited metal triple layer consisting of Ag, Cu, and Ag whose thicknesses are 200 Å each. Scan rate: 1 mV/s.

8 Evaluation of the Rate of Li Mass Transfer in the Carbon Interior. A number of studies have so far been conducted for obtaining the diffusion coefficient of Li mass transfer in graphite,[53–61] but the obtained values scatter to a great extent from 10^{-10} to 10^{-6} cm^2/s. No explanation seems to have been given for why it scatters. It appears to us that the major reason of the scattering is in the complicated nature of the electrode used for the study since the test electrodes were commonly coated-type electrodes where the powder particles of carbon active material was bound with a binder, loaded with some electric conducting additives and coated on a current collector sheet. In such an electrode there are many factors interfering with the diffusion process in question; i.e., mass transfer of solvated Li^+ in the restricted space among binder may not fast enough to realize the diffusion control, difficulty about how we define the mass transfer path in the actual carbon whose shape and size are not well-defined, electrical contact among carbon particles may differ from particle to particle, loosening of the binding action of binder may take place dur-

ing the test, the electrochemical reaction rate may not fast enough to be ignored as compared with that of Li diffusion., etc. All such factors should be taken into consideration for solving the diffusion equation, but it appears to be difficult.

Bearing in mind such issues in the coated or bound electrode, we decided to use a single fiber electrode which was picked out from a fiber felt shown in Fig. 2, where no binder, and no conductive additives are required and the shape and size is well-defined. A single straight fiber rod having a diameter of 10 μm or 8.8 μm was fixed to a Ni current collector with a carbon conductive paste and immersed in the electrolyte vertically with a depth of 5 mm. Potential step chronoamperometry (PSCA) was adopted for the determination.[36,59–61]

As already shown in Fig. 4, we could obtain a well-defined CV with a single fiber electrode. The potential step ranges were chosen by referring to the peak position due to stage formation. Prior to the rate determination experiment two cycles of CVs were recorded for making sure of the reliability of the fabricated test electrode. The measurement was performed after attaining a stationary state at the starting potential both for the insertion and the removal processes. Examples of the current decay curve are shown in Figs. 32 and 33. The curves were found to change depending on the stepping potential range. Three curves in Fig. 32 were obtained with a single carbon fiber having no surface treatment. Different from the other two curves the full line in Fig. 32 shows a current plateau, which may be ascribed to the contribution of the stage change during the progressive decrease in Li concentration. Assuming that the rate is controlled by the diffusion of Li in the fiber structure and that the process obeys the cylindrical diffusion model, we can obtain the apparent diffusion coefficient (D_{app}) by analyzing the Fick's equation for cylindrical diffusion, where the diameter of the fiber used was determined with the SEM image obtained after the measurement. The assumption

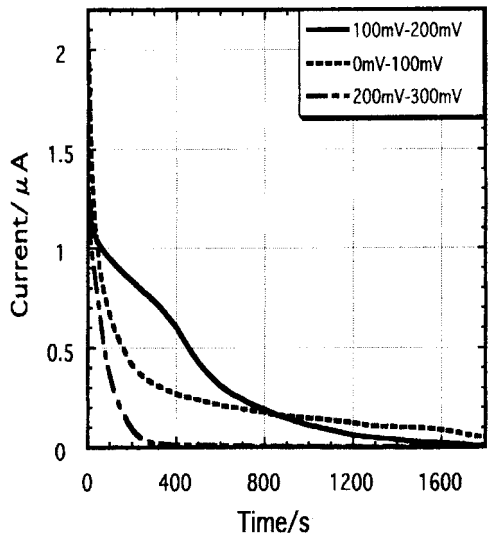

Fig. 32. PSCA decay curves of the Li deintercalation process from a pristine single fiber of well-graphitized carbon (Melblon 3100) in EC/DMC containing 1 M $LiClO_4$. The potential range inserted in the figure is potential stepping ranges, i.e., 100 mV–200 mV means to step from 100 mV to 200 mV.[36]

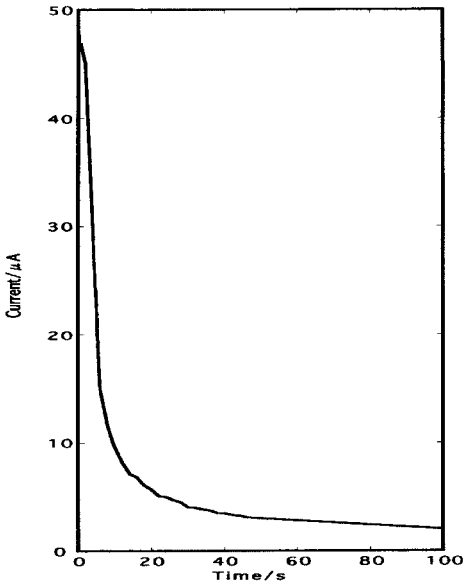

Fig. 33. PSCA decay curve of the Li deintercalation process from a 400 Å thick Ag film deposited single carbon fiber of Melblon 3100 in EC/DMC containing 1 M $LiClO_4$. The potential step range is 0–100 mV vs Li/Li^+.

that the process is controlled by diffusion is not necessarily correct since the current is influenced greatly by the charge transfer process. This is the reason why we call the obtained value as D_{app}. Figure 33 supports this argument, where we see the size of the decay current as well as the decay rate are enhanced prominently, due to the presence of a Ag film covering the fiber surface. The initial small plateau in Fig. 33 may be ascribed to the Li removal process from the covering Ag film, or the contribution of the stage change process.

The values of D_{app} depending on the stepping potential range are summarized in Fig. 34 (A) and (B) for charging and discharging processes, respectively, where the values are shown for the cases of with (●) and without (■) a vacuum-deposited Ag film. Covering with a 400 Å thick Ag film caused the D_{app} value to increase by over one order of magnitude, implying that the values do not reflect the diffusion controlled process but are controlled by the reaction rate. The values obtained after the surface treatment may still be controlled by the rate of reaction. The literature values so far reported are presumed to have the same possibility of being determined by the reaction rate and not to reflect the diffusion controlled situation. Therefore, the rate of diffusion of Li in graphite is expected to be as fast as that in liquid, or even faster than that. This argument is not unlikely since Li^+ in solution bears three or more solvent molecules due to solvation, resulting in an enlarged size and weight, while a lithium particle intercalated in the graphite layer is free from the solvent molecules, which allows for the particle to move faster.

Evaluation based on the impedance spectrometry seems unfavorable in our case because the frequency region for the evaluation of diffusion is in the range of 10^{-3} Hz, which is as slow as the direct current scan rate of 1 mV/s where any kind of electrolysis is allowed to take place at an appropriate potential and appears to have no meaning as impedance free from electrolysis.

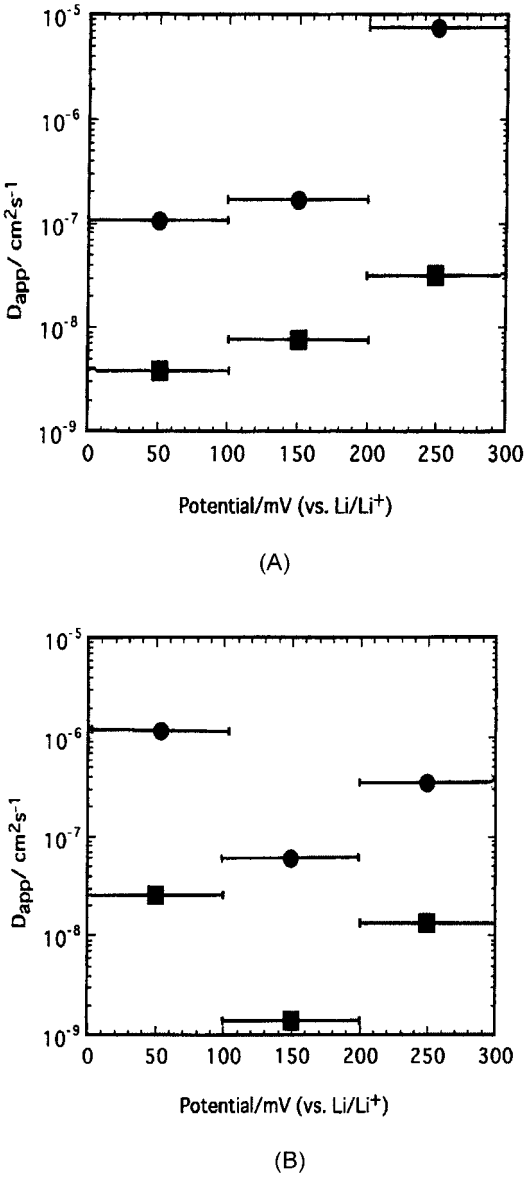

Fig. 34. Apparent diffusion coefficient D_{app} of Li determined by PSCA method for the process of insertion into (A) and extraction from (B) a well-graphitized carbon fiber (Melblon 3100) in EC/DMC containing 1 M $LiClO_4$ with (●) and without (■) a 400 Å thick Ag film deposited on the surface.[36]

9 Li Insertion/Removal Rate of Low Temperature Mesophase Carbon. We can evaluate the Li accommodation capacity in carbon from the CV. For example, the Li extraction capacity of a 800 °C mesophase disordered carbon is calculated to be 240 mAh/g from the CV in Fig. 5 (A), while that calculated based on Fig. 5 (B) amounts to 520 mAh/g in spite of the CV obtained with the same material. As recognized from this example, the capacity calculated from CV data differs depending on the potential scan rate. A similar argument holds for the evaluation under a constant current, i.e., charge/discharge capacity obtained with a high current load will give a smaller specific capacity. In order to determine the true value, it is necessary to use a CV obtained with a very slow scan rate.

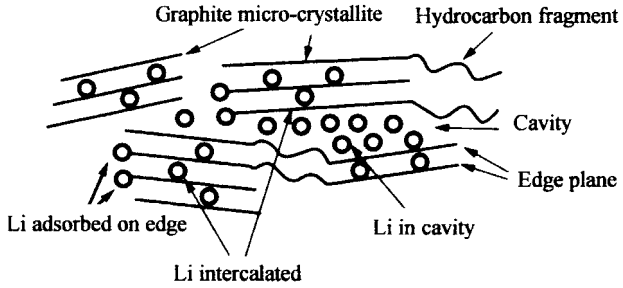

Fig. 35. Schematic presentation of the internal structure of a low temperature mesophase carbon having accommodated Li particles with various accommodation states.

On the other hand, as shown in the above example, Li accommodation capacity of low temperature carbon is very high; the extreme value so far reported is as high as 2000 mAh/g.[62] Such a high capacity is very attractive for responding to a strong demand of the advanced appliances.

There is, however, a great issue in the low temperature carbon because the rates of Li insertion/extraction are quite slow as compared to those of graphite, which cannot respond to the great demand of the advanced appliances. This is the reason that has prevented applying this material for the actual use. The high power unavailability appears essential to this material due to the past studies[63–65] and the difference in capacity depending on the scan rate as shown above supports this point of view. If this is true, the actual use of the low temperature carbon may be unlikely. The internal structure of this carbon is schematically shown in Fig. 35, where a number of micro-crystallites of graphite, like graphite embryos, are roughly oriented and connected by alkane and/or alkene chains in the matrix.[62,63] Plausible accommodation states are shown in the figure with circles, but this is only an image and has not been verified experimentally yet. The accommodation sites can be classified into two categories; i.e., intercalated ones in the micro-crystallite, and the ones outside of the micro-crystallite. The accommodation energy probably differs between the two sites, which is the cause of the appearance of two separated peaks on CV. Referring to the CVs shown in Fig. 5 we may ascribe which peak is due to the Li in micro-crystallite. As shown in Figs. 3 and 4, well-graphitized carbon reveals peaks in the potential range 0.05–0.3 V vs Li/Li^+, from which we can ascribe a peak at the lower potential in Fig. 5 to be caused by Li in the micro-crystallites, and accordingly, a broad peak in the positive potential region is ascribed to Li accommodated outside of the micro-crystallites. Under such conditions, two peaks are expected to appear on the ^7Li NMR spectrum, provided that the rate of the position exchange of Li between the two sites is slow in view of the measuring frequency, and a peak at higher energy is attributed to Li in graphite structure.

Our recent NMR study, however, has always shown only a single peak on the NMR spectrum for low temperature mesophase carbons, irrespective of the amount of Li inserted.[66] An example is shown in Figs. 36 and 37. As seen in Fig. 36, a fully charged graphite reveals a single peak due to the intercalated Li at about 45 ppm with a somewhat broad band. This single peak shifts to the lower frequency side with the lowering of the preparation temperature, reaching 18 ppm for the 600 °C

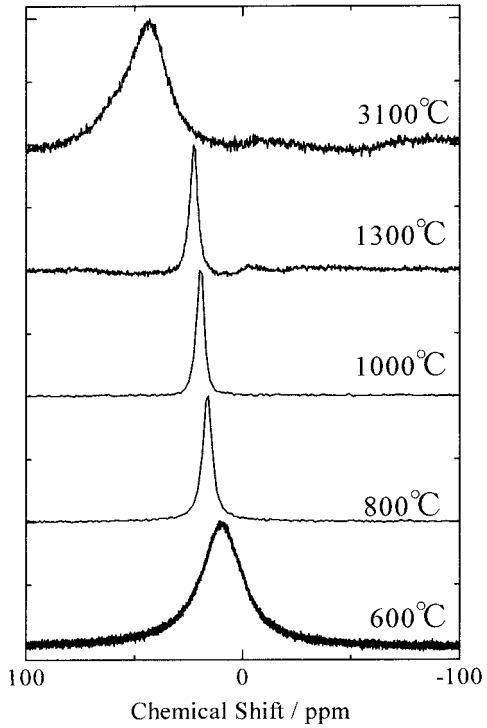

Fig. 36. ^{7}Li NMR spectra of fully charged fibers prepared at 600, 800, 1000, 1300 and 3100 °C, respectively (in EC/DMC containing 1 M $LiClO_4$).[66]

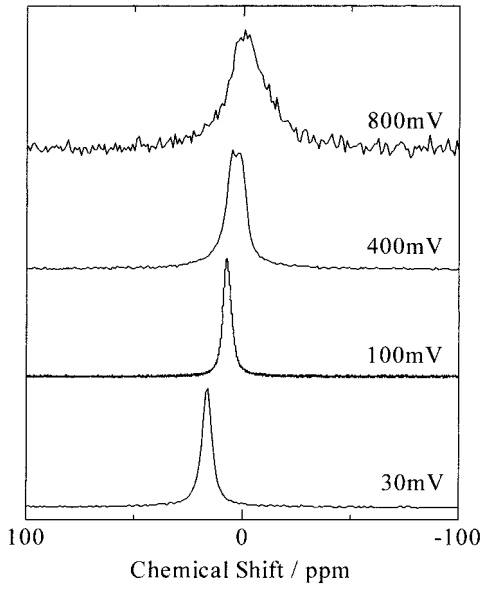

Fig. 37. ^{7}Li NMR spectra of 800 °C carbon fibers charged at 30, 100, 400 and 800 mV, in EC/DMC containing 1 M $LiClO_4$, respectively.[66]

sample. A carbon giving a single peak at about 45 ppm with fully charged Li is reasonably identified as graphite, whereas the one giving at about 10 ppm is identified as 600 °C fired carbon. Actually, a fully charged 800 °C sample gave a peak at 16 ppm. On the other hand, shifts of the peak position depending on the charged amount are shown for the 800 °C sample in Fig. 37. The peak position was found to shift from the lower side to the higher side upon increasing the charging amount of Li but it never reached 45 ppm even when fully charged. Such a tendency can be reasonably explained by assuming that basically there are two kinds of accommodations; the one is Li in the graphite-like micro-crystallites giving a peak at 45 ppm, and the other is, Li accommodated in the sites outside of the micro-crystallites giving a peak at 0 ppm, respectively. Provided that, Li accommodated in the two different sites are exchanging their positions with a frequency as fast as the NMR imposing frequency, the two peaks become merged together into one peak whose position is an algebraic average of the position of the two peaks, where a contributing weight should be taken into consideration. The weight is assumed to be proportional to the amount of Li accommodated in a specified site. Therefore, if the charging amount is low where no accommodation is expected in micro-crystallite, the resulting peak position is expected to be near 0 ppm, whereas when fully charged, the amounts in both sites are presumed to be equal from the shape of Fig. 5. The resulting peak position is expected to be about 20 ppm which is reasonably compared with the actual value of 16 ppm. Increasing the preparation temperature causes the accommodation site of micro-crystallite to exceed that of the outside sites, resulting in a positive shift in peak position, which is seen in Fig. 36.

Provided that the above mentioned assumption holds so that the internal mass transfer of Li is fast, we expect the rate of insertion/extraction of Li from and out of the low temperature carbon is essentially fast enough to meet the high power use. We are now trying to modify the surface by utilizing a single fiber electrode. The apparent diffusion coefficient obtained with a pristine fiber sample was as low as 10^{-8} cm^2/s throughout the potential region examined but we have now succeeded to enhance by about one order of magnitude, but we are still on the way for more improvement.

10 Underpotential Deposition of Li on Carbon. Studies on the underpotential deposition of a foreign metal adatom on a substrate metal have been conducted by Haissinsky,[67,68] followed by Schmidt and Gygax,[69–72] and by us,[73,74] and by Kolb.[75] We detected it optically at first by developing a specular reflection method for Cd, Pb, Tl, and Bi on a Au, Pt, and Cu electrode.[76–81] Afterwards, Itaya have studied extensively with the use of the TEM and AFM techniques until now for a number of adatoms including alkali metals deposited on a noble metal substrate. However, no studies appear to have been performed on the underpotential deposition of Li on the surface of carbon. During the course of studies to obtain CVs for active carbons in a non-aqueous electrolyte containing Li^+ we found by chance the appearance of a sharp peak at a potential a little positive to 0 V vs Li/Li^+. This was found only when the conductivity of the electrode is high with its uniform distribution over the electrode examined (Fig. 38).

We postulated that the sharp peak was caused by a Faradaic adsorption of Li on the carbon surface at a potential slightly positive to Li/Li^+ through the reaction shown below.[82]

$$C(s) + Li^+ + e^- \rightleftarrows C(s)\text{–}Li, \quad (2)$$

where C(s) means the surface of the carbon substrate, and C(s)–Li means a Li atom adsorbed by a Faradaic reduction on

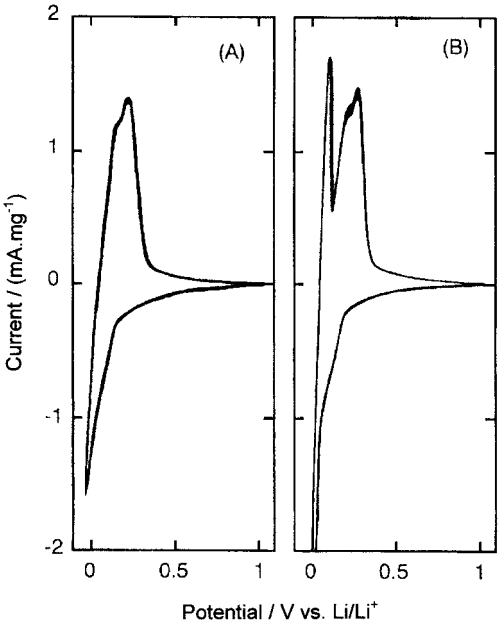

Fig. 38. CVs of a Melblon 3100 felt in EC/DMC containing 1 M $LiClO_4$ with a scan rate of 1 mV/s. (A) The electrode was fabricated as usual. (B) The electrode was fabricated with a good pressure of sandwiching with Ni expanded metals.[83]

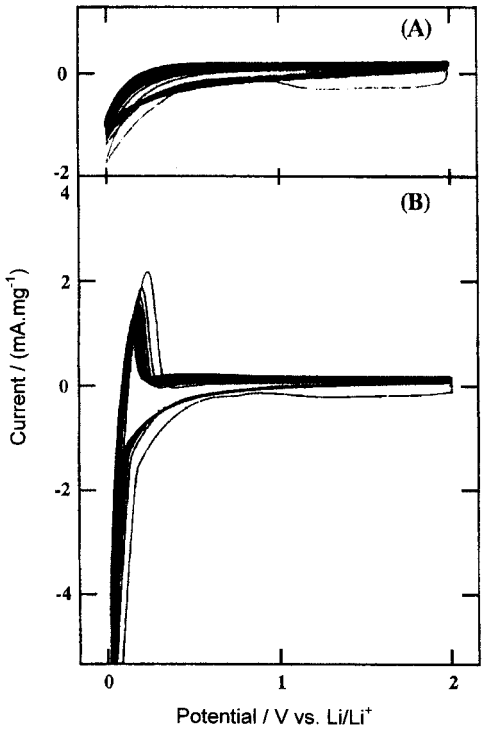

Fig. 39. CVs of a Kuractive 2500 active carbon fiber felt in PC containing 1 M $LiClO_4$ with a scan rate of 1 mV/s. Meanings of (A) and (B) are the same as in Fig. 38.[83]

the surface of the carbon substrate. The peak could be observed on any carbon irrespective of the nature of the internal structure (Fig. 39), and the peak position determined after the

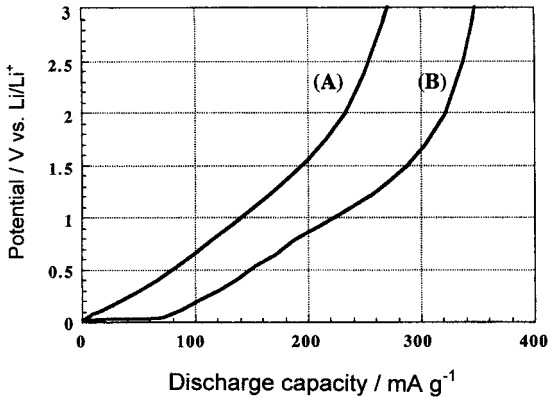

Fig. 40. Constant current discharge curves for an active carbon fiber Kuractive 2000 with 1 C rate in PC containing 1 M $LiClO_4$. The electrode fabrication is the same as in Fig. 38.[83]

Ohmic drop correction was 40 mV vs Li/Li^+. Such a phenomenon was also found for a constant discharge curve as shown in Fig. 40 for an active carbon felt electrode. An initial flat part at about 40 mV on curve (B) is attributed to the discharge of the underpotentially deposited Li.

One may be suspicious that the phenomenon is not caused by the postulated mechanism but is due to Li metal deposited on the carbon surface. The phenomenological difference between the two cases has been discussed in detail.[83]

Since the reaction is a surface reaction, the charge capacity should be proportional to the active surface area of the electrode material. Active carbon is expected to reveal a large charge capacity. The tendency was roughly proportional to the specific surface area but the difficulty arose that the surface determined by a nitrogen adsorption method was not always active enough to accept the adsorbing Li and was too narrow to accept a sufficient amount of electrolyte in the pore space. We tried to enlarge the pore opening by the method described in Section 3, and afterwards a Ag film was deposited on the surface. The resulting CV curve is shown in Fig. 41, the corresponding charge capacity being determined to be as high as 250 mAh/g.[83] Provided that the phenomenon can be reproduced very reversibly, we will have an opportunity to utilize the capacity for the rechargeable batteries as an additional capacity. The issue to be solved is how to stabilize the phenomenon and to get a stable cycleability, since it is sensitive to contaminants such as water or reducible substances contained in the electrolyte.

11 Initial Irreversible Charging Capacity and Cycleability. At the time of the first charging, any anode material requires an extra charging capacity with respect to the stationary charging capacity. This extra charge has been attributed to the formation of SEI that is formed on the anode surface from reactive entities generated as a result of the reduction decomposition of the electrolyte.[33,84] In case of a good combination between the surface of the carbon material used and the electrolyte in contact with the carbon surface, once the SEI is formed, no further electrolyte decomposition occurs in the successive charge process, since the formed SEI stabilizes the anode surface to block further decomposition as a passive film; otherwise the electrolyte will decompose endlessly at the re-

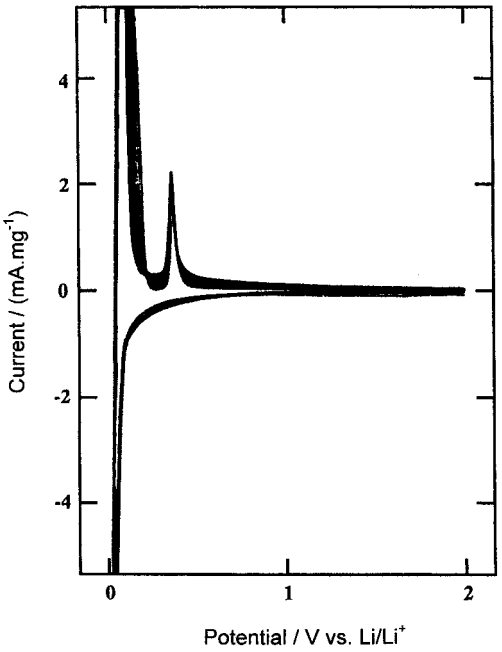

Fig. 41. CV of an active carbon fiber felt (Kuractive 2000) in PC containing 1 M $LiClO_4$. The curve was obtained with the fiber sample mildly oxidized followed by a vacuum deposition of a 500 Å thick Ag film. The scan rate: 1 mV/s.[83]

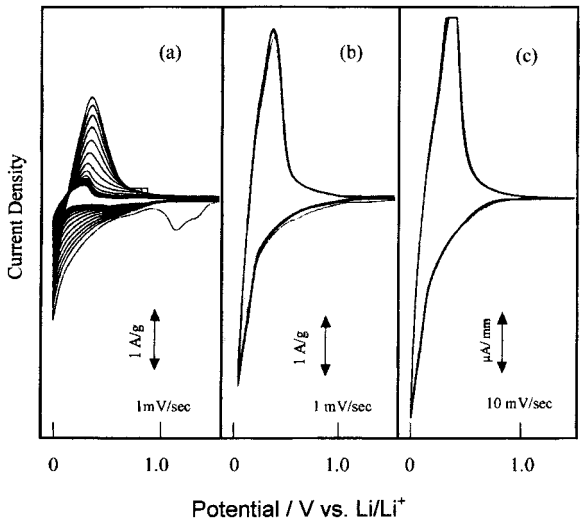

Fig. 42. CVs of well graphitized carbon fibers (Melblon 3100) in EC/DMC containing 1 M $LiClO_4$. (a) single component coated electrode on a Cu sheet with a short fiber particle bound by PVDF binder; (b) integrated fiber felt electrode sandwiched with a folded Ni expanded metal sheet and spot-welded; (c) single fiber electrode immersed vertically in the electrolyte with a depth of 5 mm from the tip.[84]

duction potential. The choice of the combination is still based on the trial-and-error method.

Minimizing the initial irreversible charging capacity (IICC) is an important task for attaining high capacity for the actual batteries, since IICC requires extra amount of the cathode material to be loaded in the cell container, which is consumed at the first charging process and never utilized for withdrawing energy in the discharging process. The size of IICC appears to be inherent to the anode material used, but we have found that the size of IICC is not fixed but varies depending on the homogeneity of the electrical conductivity even when the same material and the same electrolyte are used.[84] In Fig. 42 CVs are compared for three different electrodes where the material used was the same (Melblon 3100) for each. CV (a) was obtained with a hand made coated electrode where no conductive additives were loaded, CV (b) was with a sandwiched fiber felt, and CV (c) was with a single fiber electrode with a scan rate of 10 mV/s. In view of the homogeneity of the electrode conductivity the increase in the homogeneity is in the order of (a) $\ll$ (b) $\ll$ (c). In regard to the initial irreversibility, CV (a) reveals a marked reduction peak at around 1.2 V accompanied with a rapid decrease of the peak height during cycles, which is in contrast to CVs (b) and (c). Dependency of the IICC on the conductivity homogeneity may be elucidated based on the complicated reduction mechanism of the chemical entities generated by the reduction decomposition of the electrolyte. The entities just generated are supposed to be reactive enough to be reduced again at a different potential, resulting in the initiation of chain reaction on the surface. The polarization potential during the electrolysis is expected to be not uniform on the electrode due to an inhomogeneous conductivity distribution because resistant polarization differs from place to place, by which various kinds of chemical species may be generated, resulting in a formation of an inhomogeneous SEI which is unfavorable for perfect blocking.

The results obtained above suggest that even a coated type electrode can be improved by loading a conductive additive in the coating slurry. We attempted to verify the suggestion by incorporating 15% of Timcal 3 μm graphite flakes into the coated electrode comprised of Melblon 3100 short fibers and compared the CVs for two samples with and without the loaded conductive additive. The SEM photographs are shown for these two samples in Fig. 43, where we see the mechanical contact, i.e., the electrical contact, among the fiber particles is irregular for a single component electrode (top), while the two components-electrode loaded with graphite flakes (bottom) shows that the flakes are covering the fiber surface effectively for attaining a homogeneous conductivity distribution. The corresponding CVs are shown in Fig. 44. As clearly seen in Fig. 44, the reduction peak due to IICC on CV (a) is obviously suppressed on CV (b) which was obtained with the conductive additive loaded.

The effect of the loading of acetylene black (AB) was also examined by changing the loading amount. The results shown in Fig. 45 indicate that the peak height is increased markedly with the increase of loaded amount of AB, accompanied with some suppression of IICC. No noticeable suppression recognized in the figure is due to the superposed IICC of AB. Now we would like to compare CV (b) in Fig. 45 with that in Fig. 46, where the loaded amount of AB is the same (5%) but the mixing procedure to make slurry for coating is different. The slurry was prepared by manual mixing with an agate mortar for the former, while it was prepared by mechanical mixing for the latter. Despite the same amount of AB being loaded for Fig. 45

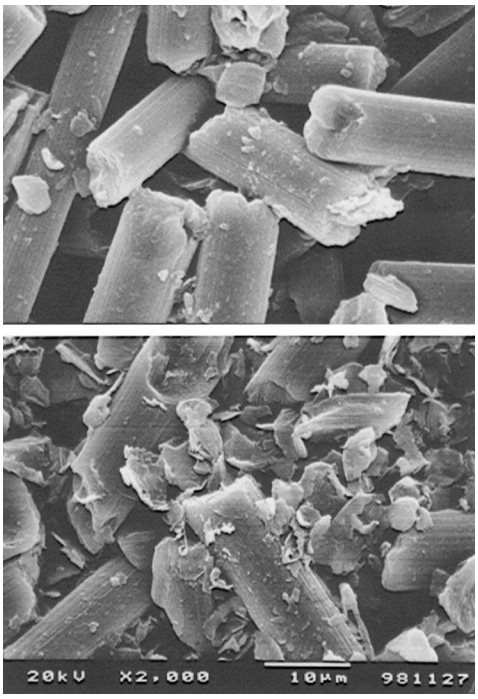

Fig. 43. SEM images of the coated electrodes of a well graphitized carbon fibers (Melblon 3100) without (top) and with (bottom) 15 wt% of graphite flakes (Timcal, average diameter: 3 μm).[84]

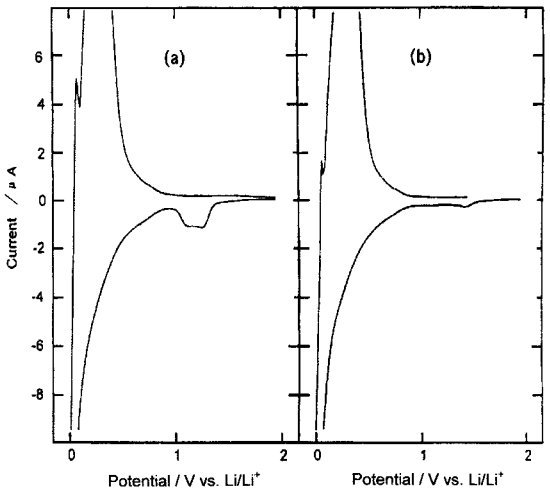

Fig. 44. CVs obtained with the electrodes corresponding graphitized carbon fibers (Melblon 3100) without (a), and with (b) 15 wt% of graphite flakes (Timcal, average diameter: 3 μm).[84]

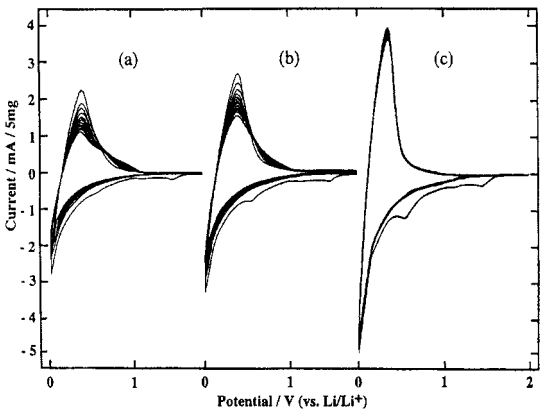

Fig. 45. CVs of a well graphitized carbon fiber (Melblon 3100) loaded with AB, in EC/DMC containing 1 M $LiClO_4$ with a scan rate of 1 mV/s. AB was loaded with a manual mixing, loading amount: (a) 2.5%; (b) 5%; (c) 10%.[84]

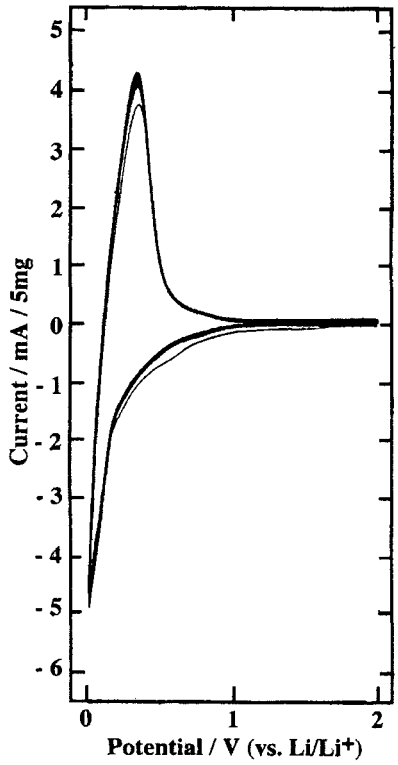

Fig. 46. CV corresponding to (b) in Fig. 45, but the mixing was done with a mechanical mixer.[84]

(b) and Fig. 46, the resulting CVs are significantly different from each other, not only enhancing the cycleability but also reducing the IICC being realized by mechanical mixing. When we refer to (A) and (B) in Fig. 47, the cause of the improvement can well be attributed to the difference in contact homogeneity. Thus, we can conclude that the electrical conductivity homogeneity is a key factor for obtaining a high performance electrode.

12 No Decomposition of PC in Contact with a Graphitized Carbon Fiber.[36, 85] PC is a good solvent for the electrolyte of Li-ion batteries in view of the high conductivity even at low temperature and the low price, but it has a serious problem because it is decomposed vigorously when it is in contact with graphitized carbons at a negative potential. The decomposition has been believed to be due to the solvent co-intercalation during the charging of the anode.[86] Such a vigorous decomposition was found for a well graphitized integrated fiber felt (Melblon 3100) as well, which is shown in Fig. 48. The fiber felt sandwiched with a folded Ni expanded metal whose

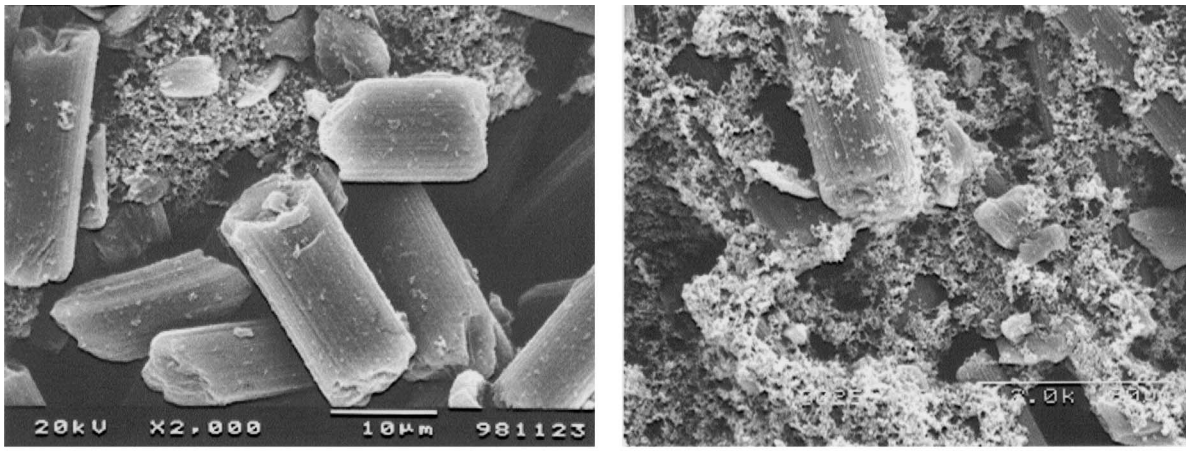

Fig. 47. SEM images of coated electrodes comprised of a well graphitized carbon fiber (Melblon 3100) loaded with 5 wt% of AB. The coating slurry was prepared by manual mixing for (A), and by mechanical mixing for (B) where homogeneous dispersion of AB is clearly seen.[84]

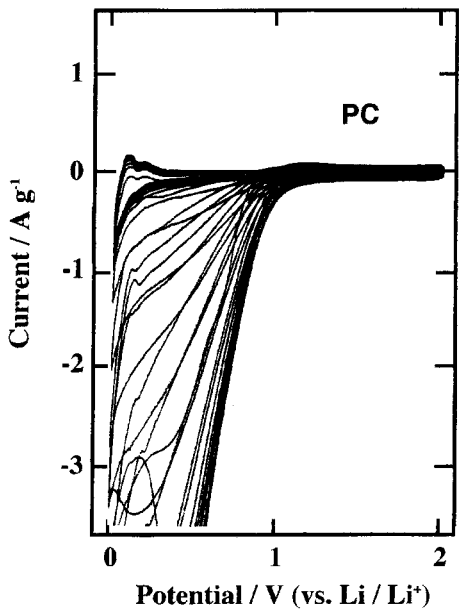

Fig. 48. CV of an integrated fiber felt of a well-graphitized carbon fiber in PC containing 1 M $LiClO_4$.[85]

rims were spot-welded at several points tightly was destroyed by expansion after 20 cycles repetition, indicating that the phenomenon appears to be essential.

During the course of measurements using a single fiber electrode, however, we found by chance that PC did not decompose even in contact with a well-graphitized fiber. CVs obtained in the electrolytes of EC/DMC and PC are shown in Fig. 49, where we find very stable CVs in both cases with no detectable IICC even in PC. This is very surprising and we repeated and repeated the experiment many times. As a result, we found sometimes an indication of the decomposition. Precise examination has showed that the decomposition tends to occur when the fiber was not straight or mounted not symmetrically against the counter electrode, for example, in the case where the distance from the counter electrode differs between the tip and the part near the liquid level.

The second experiment was to examine a test electrode fabricated with a bundle of five fibers which were fixed to the wall of a thin Ni wire at the tip. Two cases were examined: i.e., all the fibers were fixed with a vertical uniform direction, and all the fibers were bundled randomly. Results obtained with these two kinds of bundles are shown in Fig. 50. In the case of a uniform fiber direction, the obtained CV was relatively stable though not well defined, while the electrode with randomly arranged fibers caused the electrolyte to decompose.

Summarizing the results, we can conclude that the PC decomposition does not take place even on a graphite electrode whenever the conductivity of the electrode is sufficiently high, uniformly distributed, and the Ohmic drop between the test and the counter electrodes during the electrolysis is kept uniform over the electrode surface. As already pointed out in Section 11, formation of a uniform and compact SEI is the most important factor to minimize IICC. Since IICC is due to the initial solvent decomposition, a condition to attain a minimized IICC appears to be related to preventing the PC decomposition. This postulate seems to be not in accordance with the PC decomposition mechanism now accepted. Detailed investigation based on the chemistry of SEI in relation to the reaction active site will be helpful for drawing the conclusions for acceptable mechanisms.

13 Improving the Performance by Making a C/C Composite.[87–89] Having demonstrated the effect of uniform conductivity distribution, the authors would like to provide an effective practical method for realizing the conductivity uniformity. As the test sample we chose a low temperature carbon, since the cycleability is poor as compared to graphitized carbons. At present, almost all the conventional coated electrodes are fabricated by loading a conductive additive by which the

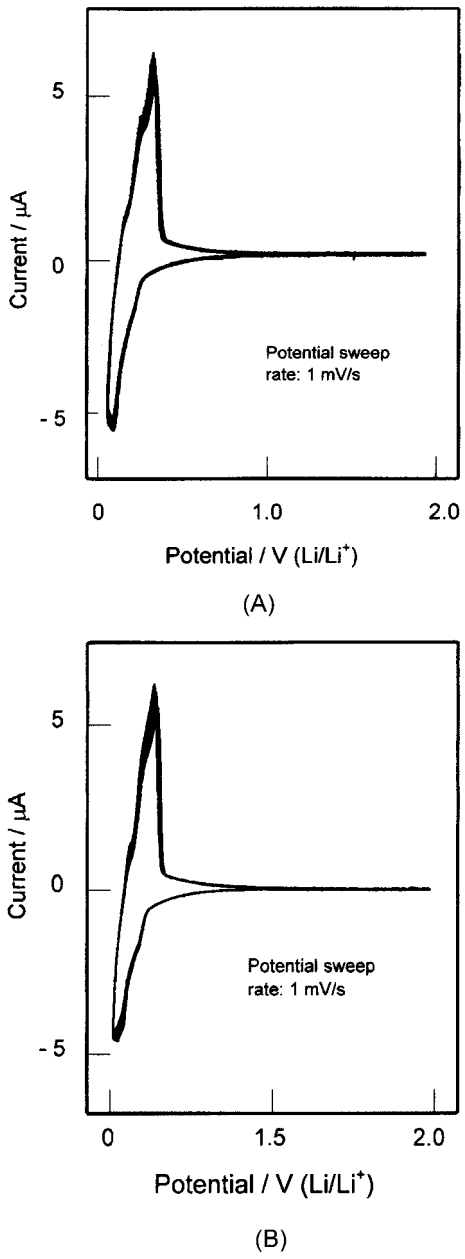

Fig. 49. CVs of a single fiber of a well-graphitized carbon (Melblon 3100) in EC/DMC (A), and PC (B), the salt dissolved being 1M $LiClO_4$. The scan rate was 1 mV/s for both.[36,85]

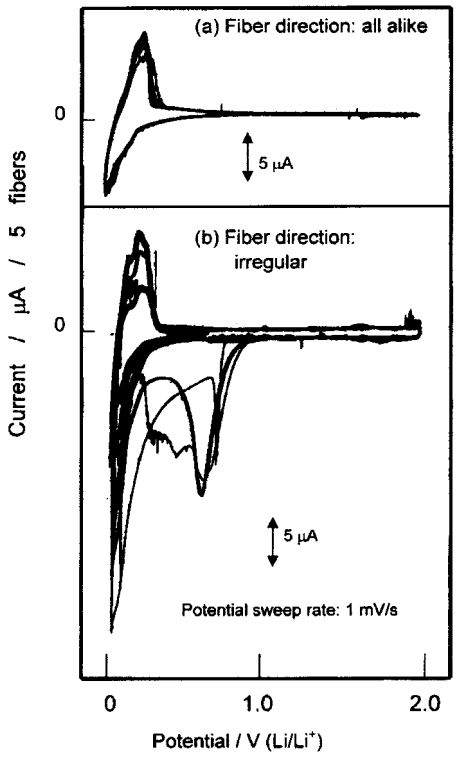

Fig. 50. CVs of a five fibers bundled electrode comprised of well-graphitized carbon fibers (Melblon 3100) in PC containing 1 M $LiClO_4$. (a) all the fibers were fixed with a vertical uniform direction; (b) all the fibers were bundled randomly.[85]

electrical contact of each active material particle is facilitated. The contact, however, is still taken by a simple mechanical contact of solid to solid, implying that the state is far from the ideal one. Our idea is to make a C/C composite where the particles of carbon active material are bound together with a conductive carbon through a chemical bond. Mesophase carbon fiber felt prepared at 950 °C was selected as the active material. The method for making a C/C composite was based on utilizing a thermosetting resin. At first, the fiber felt sample was immersed in the solution of a thermosetting resin, cured, and pyrolyzed into conductive carbon in an inert atmosphere. As the thermosetting resin we selected two resins: i.e., epoxy resin and phenol resin. After examining the incorporating, curing, and pyrolyzing conditions, we could obtain the most preferable conditions for two resins. SEM images of the C/C composite thus obtained are shown in Fig. 51. Epoxy resin was too hard for itself to creep on the fiber surface during the pyrolysis giving a rigid binding of rugged surface. In contrast, resol (a kind of phenol resin) gave a C/C having a very smooth surface and all the fibers appear to be bound by resol carbon very tightly. A constant current cycle test with 1.5 C rate was applied to both of the C/C composites in PC containing 1 M $LiClO_4$. The results obtained with these C/C composites are shown in Fig. 52, where the result with a pristine fiber felt is shown for comparison. The cycleability was improved markedly by making the C/C composite. Especially, as inferred from the appearance of the SEM image, resol showed the most significant improvement.

One may expect that the C/C composite method can be applied to the high temperature carbon fiber. We examined how to make C/C composite by applying resol to a graphitized fiber. The results were compared with those of pristine. Not only the peak height of the deintercalation peak but also the cycleability were improved. An additional effect is the appearance of a sharp peak due to the underpotential deposition of Li, which has been explained in Section 10. The enhanced IICC in the case of b) is due to the carbon formed from resol. Results obtained with C/C composite are also in accordance with the postulated concept that the homogeneity of high conductivity of the electrode provides a good performance.

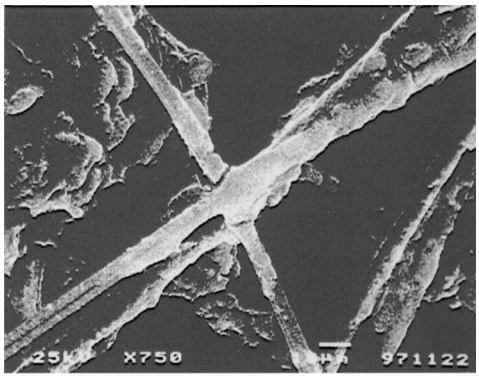

(A)

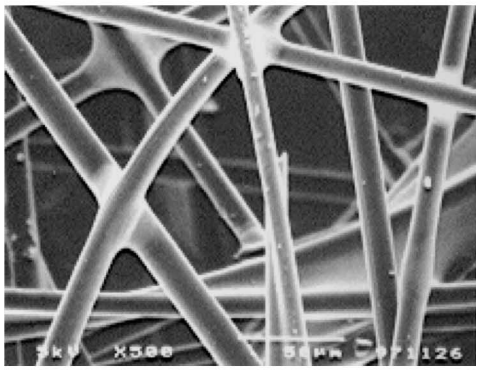

(B)

Fig. 51. SEM images of the C/C composites prepared by the pyrolysis of the resins binding the carbon fibers of mesophase low temperature carbon obtained at 950 °C. (A) Epoxy resin was pyrolyzed up to 900 °C. (B) Resol resin was pyrolyzed at 800 °C.[89]

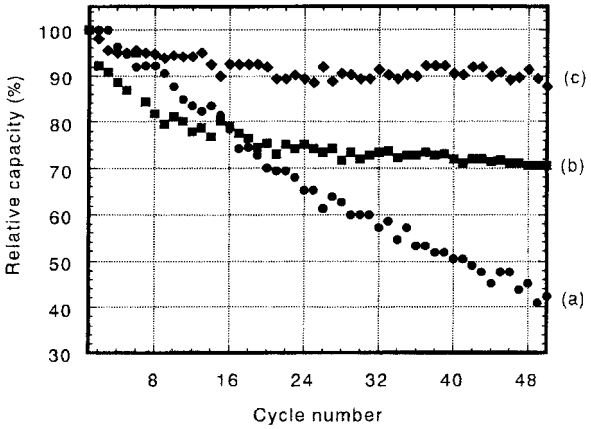

Fig. 52. Capacity fading during the constant current charge/discharge cycle test with 1.5 C rate both for charging and discharging for pristine felt of 950 °C prepared carbon fiber (a), the C/C composite prepared with epoxy resin (b), and the C/C composite with resol resin (c).[87–89]

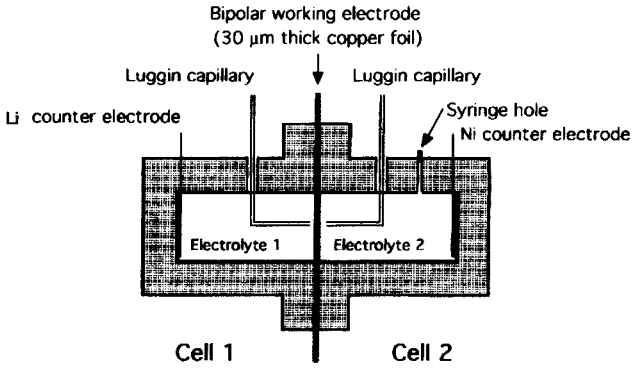

Fig. 53. A bipolar cell constructed for verifying Li mass transfer through a centering metal foil.[90]

14 Free Movement of Li in a Solid Metal at an Ambient Temperature.[35,90] As already pointed out in Section 4 and related sections we believe that Li particle moves freely in a metal film deposited on the surface of carbon fiber. Such a concept, however, has been facing to objection at academic meetings, resulting in no acceptance for publication in a scientific journal. This stimulated us to find acceptable pieces of evidence for proving the phenomenon. For the purpose of verification, we decided to fabricate a bipolar cell where a metal foil is sandwiched by two identical electrolysis cells facing each other and the foil is used as a working electrode (Fig. 53). The verification procedure is as follows: In Cell 1 an electrolyte containing Li^+ is filled, and that containing no Li^+ is filled in Cell 2, then the centering bipolar electrode is polarized in Cell 1 at a sufficiently negative potential but positive than that of Li deposition, and polarized at more positive potential in Cell 2. While both sides are polarized, an aliquot of the electrolyte in Cell 2 is pipetted out from time to time the for atomic absorption analysis of Li. If we detect the increasing amount of Li in Cell 2 after polarization this will be the direct confirmation of Li mass transfer through a metal foil. Of course, absence of pinholes should be confirmed in advance by vacuum test.

As the sample metal we selected a Cu foil because Cu is reported to form no alloy with Li at an ambient temperature, since many researchers did not accept our concept of Li free mass transfer for a metal forming no alloys with Li. The results obtained with a Cu foil are shown in Fig. 54 where a linear increase in Li concentration with time is clearly seen after the start of polarization. We succeeded to publish the paper in the beginning of the last year.[90] As seen clearly in the figure, the Li concentration in Cell 2 was kept near zero level before the polarization, which is an indicative of no pinhole that would allows spontaneous leakage of Li. Results obtained with a Ag foil were presented but are still being cast doubt by the audience.[91] Amperometric method enables one to determine the diffusion coefficient of Li in metal, by which we could obtain the potential dependency profile of the diffusion coefficient. The values were in the range of 10^{-7} to 10^{-6} cm^2/sec. We are now testing with the other metals and trying to ob-

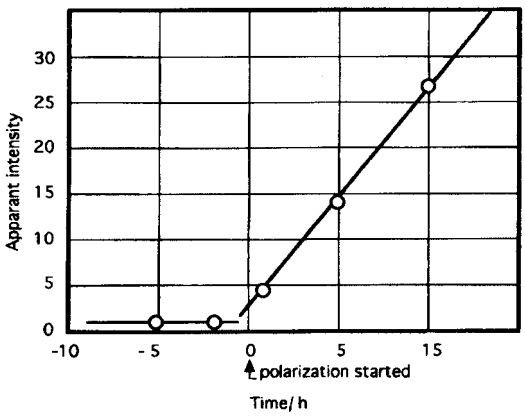

Fig. 54. Time dependency of the Li ion concentration (as expressed as relative intensities of atomic absorption) of the electrolyte in Cell 2.

tain a relationship between the applied potential and the Li concentration in the metal during the polarization.

Conclusive Remarks

Due to the restriction of the given space, many other interesting results so far obtained have to be put aside in this article, but the author will be very glad if the readers are interested in some items described here. Our study is not concerned with the synthesis of carbonaceous materials but restricted in evaluation in view of modifying the carbon surface. Through a thorough examination of the modified surface the author believes one will be able to infer the internal structure of carbon. Carbon is a very old material but at the same time a very new material. The author believes it is important even for scientists to remind the old saying that "By exploring the old, one becomes able to understand the new".

The author would like to extend the present study in the following items:

(1) Experimental and theoretical confirmation of mass transfer of Li in solid metals other than Ag and Cu.

(2) Verification of hopping of Li particle across a gap between two neighboring layers, i.e., as already seen in Figs. 15 and 17 a metal film deposited on the surface of a carbon fiber appears not bound tightly to the substrate, otherwise it could not be removed so easily, which implies that there is a gap between the carbon and the metal film. In spite of the loose contact, Li showed the evidence of free mass transfer throughout the entire pathway. We would like to make clear the mechanism of such free mass transfer.

(3) Confirmation of a free Li movement like the tunneling effect through a retarding skin. This is based on the fact that, despite the presence of a compact oxide layer on a metal foil, we have found that Li moves freely across the layer.

(4) The author would like to propose a new term "Carbon alloy" which will be prepared by nano-technology tools with a variety of elements. The new material of carbon alloy is believed to contribute to support the advanced material technology in the new century.

The author's sincere thanks are due to my colleagues who devoted their important times for studying the carbon science and technology with me until now. The present results would have not been obtained without the studies of my colleagues. The author acknowledges deeply Professor Kyoichi Sekine, Mrs. Chieko Nakahara, Professor Yuria Saito, Dr. Hiroshi Kataoka, Mr. Masamichi Nagashima, Mr. Tetsuya Mine, Mr. Hajime Amano, Miss Masako Takayama, Mr. Itaru Tamura, Mr. Masahiro Kikuchi, Mr. Jun Ebana, Mr. Hidekazu Awano, Mr. Tetuya Ura, Mr. Jupei Yoshida, Mr. Ryosuke Takagi, Mr. Atsushi Shimoyamada, Mr. Koji Sumiya, Mr. Koji Okubo, Miss Miyoko Yashiro, Miss Miyuki Uratani, Mr. Ryoichi Takasu, Mr. Junji Suzuki, Mr. Takayuki Katusta, Mr. Morihiro Saito, Mr. Chikayoshi Yamada, Mr. Keita Yamaguchi, Mr. Msaomi Yoshida, Mr. Fuminori Mouri, Mr. Yohichiiro Nishijima, Mr. Sigehiro Tamura, Mr. Ken Tekuramori, Mr. Wataru Omae, Mr. Nobuaki Kikuchi Mr. Atsushi Shimokawa, Mr. Satoshi Aoki, Shigeki Ohara, and Mr. Takashi Igarashi for their excellent collaboration in pursuing the present studies.

The author would like to acknowledge Oukazaidan, Iketani Zaidan, Yazaki Zaidan, Mitubishi Zaidan, and PEC fund of MITI, Japan for their financial support of our work.

References

1 Wendell M. Latimer, "The Oxidation States of The Elements and Their Potentials in Aqueous Solutions," 2nd ed, Prentice-Hall, Englewood Cliffs, N.J. (1956) Chap. 23.

2 "Handbook of Batteries," ed by David Linden, 2nd ed, McGraw-Hill, New York (1995), Chap. 36.

3 "Handbook of Batteries," ed by David Linden, 2nd ed, McGraw-Hill, New York (1995), pp. 36.22–26.24.

4 "Rechargeable Lithium and Lithium-Ion Batteries," ed by Sid Megahed, Brian M. Barnett, and Like Xie, Proceedings, Vol. 94-28, The Electrochem. Soc., Inc., Pennington, N.J. (1995).

5 "Materials for Electrochemical Energy Storage and Conversion-Batteries, Capacitors, and Fuel Cells," ed by Daniel H. Doughty, Brijesh Vyas, Tsutomu Takamura, and James R. Huff, Symposium Proceedings, Vol. 393, Material Research Soc. Pittsburgh, Penn. (1995), Part VII.

6 "Materials for Electrochemical Energy Storage and Conversion-Batteries, Capacitors, and Fuel Cells," ed by David S. Ginley. Daniel H. Doughty, Bruno Scorsati, Tsutomu Takamura, and Zhengming Zhang, Material Research Society, Symposium Proceedings Vol. 496 Material Research Soc. Pittsburgh, Penn. (1998) Part IV-VI.

7 "Intercalation Compounds for Battery Materials," ed by G. A. Nazri, M. Thacckeray, and T, Ohzuku, Proceedings Vol., 99-24 The Electrochemical Soc. Inc., Pennington, N. J. (2000).

8 "Lithium Batteries," ed by S. Surampudi, R. A. Marsh, Z. Ogumi, and J. Prakash, Proceedings Vol. 99-25, The Electrochemical Soc. Inc., Pennington, N. J. (2000).

9 "Proceedings of the Eighth International Meeting on Lithium Batteries," ed by O. Yamamoto, Z. Ogumi, and M. Morita, Elsevier Science S.A., Amsterdam (*J. Power Sources*, **68**,**1-2**) (1997).

10 "Proceedings of the Ninth International Meeting on Lithium Batteries," ed by Peter G. Bruce, John T.S. Irvine, and Colin A. Vincent, Elsevier Science S.A., Amsterdam (*J. Power Sources*, **81**, **82**) (1999).

11 "Handbook of Battery Materials," ed by Jürgen O. Besenhard, WILEY-VCH, Weinheim (1999), Part III, Chapters 2–8.

12 P. Liu, G. L. Hornyak, A. C. Dillon, T. Gennett, M. J. Heben, and J. A. Turner, in "Lithium Batteries," ed by S. Surampudi, R. A. Marsh, Z. Ogumi, and J. Prakash, Proceedings Vol., 99-25, The Electrochemical Soc. Inc., Pennington, N. J. (2000), p. 31.

13 S. Yata, H. Kinoshita, M. Komori, N. Ando, T. Kashiwamura, T. Harada, K. Tanaka, and T. Yamabe, *Synth. Met.*, **62**, 153 (1994).

14 K. Sato, M. Noguchi, A. Demachi, N. Oki, and M. Endo, *Science*, **264**, 556 (1994).

15 J. R. Dahn, T. Zheng, Y. Liu, and J. S. Xue, *Science*, **270**, 590 (1995).

16 M. Hara, A. Satoh, N. Takami, and T. Ohsaki, *J. Phys. Chem.*, **99**, 16338 (1995).

17 A. Mabuchi, K. Tokumitsu, H. Fijimoto, and T. Kasuh, *J. Electrochem. Soc.*, **142**, 1041 (1995).

18 T. Zheng, Y. Liu, E. W. Fuller, S. Tseng, U. von Sacken, and J. R. Dahn, *J. Electrochem. Soc.*, **142**, 2581 (1995).

19 H. Higuchi, K. Uenae, and A. Kawakami, *J. Power Sources*, **68**, 212 (1997).

20 K. Tatsumi, T. Kawamura, S. Higuchi, T. Hosotsubo, H. Nakajima, and Y. Sawada, *J. Power Sources*, **68**, 263 (1997).

21 N. Takami, A. Satoh, T. Ohsaki, and M. Kanda, *J. Electrochem. Soc.*, **145**, 478 (1998).

22 H. Azuma, H. Imoto, S. Yamada, and K. Sekai, *J. Power Sources*, **81-82**, 1 (1999).

23 J. R. Dahn, *Phys. Rev. B*, **44**, 9170 (1991).

24 T. Ohzuku, Y. Iwakoshi, and K. Sawai, *J. Electrochem. Soc.*, **140**, 2490 (1993).

25 M. Inaba, H. Yoshida, Z. Ogumi, T. Abe, Y. Mizutani, and M. Asano, *J. Electrochem. Soc.*, **142**, 20 (1995).

26 M. Winter and J. O. Besenhard, in "Handbook of Battery Materials," ed by Jürgen O. Besenhard, WILEY-VCH, Weinheim (1999), p. 391.

27 T. Noda and M. Inagaki, *Bull. Chem. Soc. Jpn.*, **37**, 1534 (1964).

28 A. Oberlin and G. Terriere, *Carbon*, **13**, 367 (1975).

29 G. M. Jenkins and K. Kawamura, "Polymeric Carbons," Cambridge University Press, (1976) p. 68.

30 E. Peled, *J. Electrochem. Soc.*, **126**, 2047 (1979).

31 E. Peled, in "Lithium Batteries," ed by J. P. Gabano, Academic Press, (1983), p. 43.

32 D. Aurbach, A. Zaban, Y. Ein-Eli, I. Weissman, O. Chusid, B. Markovsky, M. Levi, E. Levi, A. Schechter, R. Granot, *J. Power Sources*, **68**, 91 (1997).

33 E. Peled, G. Golodnitsky, and J Penciner, in "Handbook of Battery Materials," WILEY-VCH, Weinheim (1999), pp. 419-456.

34 M. Winter and J. O. Besenhard, in "Handbook of Battery Materials," ed by Jürgen O. Besenhard, WILEY-VCH, Weinheim (1999), p. 395.

35 J. Suzuki, Thesis of Master Degree, "Mechanism of the Improvement of Li Doping/Undoping Characteristics of Graphitized Carbon Fibers Covered with a Vacuum Deposited 11 Group Metal Film," Department of Chemistry, Rikkyo University (1999).

36 K. Yamaguchi, Thesis of Master Degree, "Evaluations of Li Doping/Undoping Characteristics of Graphitized Carbon Materials for Li-ion Secondary Batteries by the Use of a Single Carbon Fiber Electrode," Department of Chemistry, Rikkyo University (2000).

37 M. Uratani, R. Takagi, K. Sumiya, K. Sekine, and T. Takamura, *Denki Kagaku*, **66**, 1146 (1998), M. Uratani, Graduation Thesis, "In Situ Microscopic Observation of a Carbon Fiber during the Electrochemical Doping/Undoping of Lithium," Department of Chemistry, Rikkyo University (1998).

38 T. Katsuta, Thesis of Master Degree, "Li Doping/Undoping Reaction in Mesophase Low Temperature Carbon Material," Department of Chemistry, Rikkyo University (1999).

39 M. Kikuchi, Y. Ikezawa, and T. Takamura, *J. Electroanal. Chem.*, **396**, 451 (1995).

40 T. Takamura, M. Kikuchi, H. Awano, T. Ura, and Y. Ikezawa, in "Materials for Electrochemical Energy Storage and Conversion-Batteries, Capacitors, and Fuel Cells," ed by David S. Ginley. Daniel H. Doughty, Bruno Scorsati, Tsutomu Takamura, and Zhengming Zhang, Symposium Proceedings, Vol. 496, Material Research Soc., Pittsburgh, Penn. (1995) pp. 345–355.

41 T. Takamura, H. Awano, T. Ura, and K. Sumiya, *J. Power Sources*, **68**, 114 (1997).

42 S. Tamura, Graduation Thesis, "Improvement of Characteristics of Active Carbon Fibers by Surface Modification of Electric Double Layer Capacitors," Department of Chemistry, Rikkyo University, (1999).

43 R. Takagi, K. Okubo, K. Sekine, and T. Takamura, *Denki Kagaku*, **66**, 333 (1997).

44 T. Takamura, K. Sumiya, J. Suzuki, C. Yamada, and K. Sekine, *J. Power Sources*, **81-82**, 368 (1999).

45 T. Takamura, K. Sumiya, Y. Nishijima, J Suzuki, and K. Sekine, in "Materials for Electrochemical Energy Storage and Conversion-Batteries, Capacitors, and Fuel Cells," ed by David S. Ginley. Daniel H. Doughty, Bruno Scorsati, Tsutomu Takamura, and Zhengming Zhang, Symposium Proceedings, Vol. 496, Material Research Soc., Pittsburgh, Penn. (1998) pp. 557-562.

46 M. Saito, Private communication, Department of Chemistry, Rikkyo University (1999).

47 K. Nishimura, H. Honbo, S. Takeuchi, T. Horiba, M. Oda, M. Koseki, Y. Muranaka, Y. Kozono and H. Miyadera, *J. Power Sources*, **68**, 436 (1997) ; H. Honbo, S. Takeuchi, H. Momose, K. Nishimura, T. Horiba, Y. Muranaka and Y. Kozono, *Denki Kagaku*, **66**, 939 (1998).

48 K. Sumiya, J. Suzuki, R. Takasu, K. Sekine, and T. Takamura, *J. Electroanal. Chem.*, **462**, 150 (1999).

49 Y. Idota, T. Kubota, A. Matsufuji, Y. Mekawa, and T. Miyasaka, *Science*, **276**, 1395 (1997).

50 T. Takamura, J. Suzuki, C. Yamada, K. Sumiya, and K. Sekine, *Surface Engineering*, **15**, 225 (1999).

51 M. Yoshida, Thesis for Master Degree, "Relationship between the Surface Condition and the Rate of Li Insertion/Extraction Reaction at the Highly Graphitized Carbon Fiber Electrode," Department of Chemistry, Rikkyo University (2000).

52 M. Yoshida, J. Suzuki, K. Sekine, and T. Takamura, Presented at the 39th Battery Symposium in Japan, November 25–27, Sendai, Japan (1998), Abstract, pp. 457–458.

53 T. F. Fuller, M. Doyle, and J. S. Newman, *J. Electrochem. Soc.*, **141**, 1 (1994).

54 N. Takami, A. Satoh, M. Hara, and T. Ohsaki, *J. Electrochem. Soc.*, **142**, 371 (1995).

55 T. Uchida, Y. Morikawa, H. Ikuta, M. Wakihara, and K. Suzuki, *J. Electrochem. Soc.*, **143**, 2606 (1996).

56 R. Yazami, M. Dechamps, S. Genies, J. C. Frison, *J. Power Sources*, **68**, 110 (1997).

57 D. Aurbach, A. Zaban, Y. Ein-Eli, I. Weissman, O. Chusid, B. Markovski, M. Levi, E. Levi, A. Schechter, and E. Granot, *J. Power Sources*, **68**, 95 (1997).

58 A. Funabiki, M. Inaba, T. Abe, and Z. Ogumi, *J. Electrochem. Soc.*, **146**, 2443 (1999).

59 K. Yamaguchi, R. Takagi, K. Sekine, and T. Takamura, Presented at the 39th Battery Symposium in Japan, November 25–27, Sendai, Japan (1998), Ext. Abstr. pp. 421–422.
60 K. Yamaguchi, R. Takagi, J. Suzuki, K. Sekine, and T. Takamura, Presented at the 40th Battery Symposium in Japan, November 14–16, Kyoto, Japan (1999), Ext. Abstr. pp. 397–398.
61 K. Yamaguchi, J. Suzuki, K. Sekine, and T. Takamura, Presented at the 50th ISE Meeting in Pavia, Italy, September 3–7 (1999).
62 M. Winter and J. O. Besenhard, in "Handbook of Battery Materials," ed by Jürgen O. Besenhard, WILEY-VCH, Weinheim (1999), p. 398.
63 T. Zheng and J. R. Dahn, *J. Power Sources*, **68**, 201 (1997).
64 N. Takami, A. Satoh, T. Ohsaki, and M. Kanda, *Electrochim. Acta*, **42**, 2537 (1997).
65 N. Takami, A. Satoh, M. Hara, and T. Ohsaki, *J. Electrochem. Soc.*, **145**, 478 (1998).
66 H. Kataoka, Y. Saito, O. Omae, J. Suzuki, K. Sekine, and T. Takamura, Presented at the 41st Battery Symposium in Japan, November 20–22, Nagoya, Japan (2000), Ext. Abstr. pp. 616–617.
67 M. Haissinsky, *J. Chem. Phys.*, **32**, 116 (1935).
68 M. Haissinsky and J. Danon, *J. Chem. Phys.*, **48**, 106 (1958).
69 K. Schmidt and H. R. Gygax, *J. Electroanal. Chem.*, **12**, 300 (1966) ; **13**, 378 (1966) ; **14**, 126 (1967).
70 K. Schmidt and N. Württhrich, *J. Electroanal. Chem.*, **28** 349 (1970) ; **34**, 377 (1972) ; **40**, 399 (1972).
71 K. Schmidt and H. R. Gygax, *Helv. Chim. Acta*, **48**, 1178, 1554 (1965) ; **49**, 733, 1105 (1966).
72 B. J. Bowles, *Electrochim, Acta*, **10**, 717, 731 (1965) ; **15**, 589, 737 (1970).
73 F. Mikuni and T. Takamura, *Denki Kagaku*, **37**, 852 (1969).
74 F. Mikuni and T. Takamura, *Denki Kagaku*, **38**, 113 (1970) ; **39**, 237, 579 (1971).
75 D. N. Kolb, N. Przasnyski, and H. Gerischer, *J. Electroanal. Chem.*, **54**, 25 (1975).
76 T. Takamura, K. Takamura, W. Nippe, and E. Yeager, *J. Electrochem. Soc.*, **117**, 625 (1970).
77 U. Moriyama and T. Takamura, *Denki Kagaku*, **40**, 300 (1972).
78 T. Takamura and Y. Sato, *J. Electroanal. Chem.*, **41**, 31 (1973) ; **47**, 245 (1973).
79 T. Takamura, F. Watanabe, and K. Takamura, *Electrochim. Acta*, **19**, 933 (1974).
80 F. Watanabe, K. Takamura, and T. Takamura, *Denki Kagaku*, **43**, 469 (1975) ; **45**, 689 (1977).
81 K. Takamura, F. Watanabe, T. Takamura, *Electrochim. Acta*, **26**, 979 (1981).
82 T. Takamura, H. Awano, R. Takasu, K. Sumiya, and K. Sekine, *J. Electroanal. Chem.*, **455**, 223 (1998).
83 R. Takasu, K. Sekine, and T. Takamura, *J. Power Sources*, **81-82**, 224 (1999).
84 T. Takamura, M. Saito, A. Shimokawa, C. Nakahara, K. Sekine, S. Maeno, and N. Kobayshi, *J. Power Sources*, **90**, 45 (2000).
85 K. Yamaguchi, J. Suzuki, M. Saito, K. Sekine, and T. Takamura, *J. Power Sources*, in press (2001).
86 M. Winter and J. O. Besenhard, in "Handbook of Battery Materials," ed by Jürgen O. Besenhard, WILEY-VCH, Weinheim (1999), p. 396.
87 M. Saito, Thesis for Master Degree, "Study of the Carbon Anode Having Higher Charge/Discharge Performances for Lithium-ion Secondary Batteries," Department of Chemistry, Rikkyo University (1999).
88 M. Saito, K. Sumiya, K. Sekine, and T. Takamura, *Electrochemistry*, **67**, 957 (1999).
89 M. Saito, K. Yamaguchi, K. Sekine, and T. Takamura, *Solid State Ionics*, **135**, 199 (2000).
90 J. Suzuki, M. Yoshida, C. Nakahara, K. Sekine, M. Kikuchi, and T. Takamura, *Electrochem. Solid-State Letters*, **4**, A1 (2001).
91 J. Suzuki, K. Sekine, and T. Takamura, Presented at the 68th Meeting of the Electrochem. Soc. Japan, April 1–3, Kobe, Japan (2001).

Tsutomu Takamura: 1930 May 5, Born in Tokyo, Japan. 1953, Graduated from Tohoku University (Department of Chemistry, Faculty of Science). 1958, Finished the post graduation course at the Department of Chemistry of Tohoku University. 1958, Obtained the Degree of Dr. of Science from Tohoku University with the thesis of "Calorimetric Study of Silica Gel–Benzene Adsorption System". 1958, Jointed to Tokyo Shibaura Electric Company (Now Toshiba) Mazda Research Lab. 1968, Postdoctoral Research Associate at Case Western Reserve University, Department of Chemistry, Professor Ernest B. Yeager's Laboratory. 1978, General Manager of Chemical Laboratory, Toshiba R&D Center. 1984, President of Toshiba Research Consulting Corporation, Ltd. 1989, Professor of Rikkyo (St Paul's) University (major in physical chemistry). 1990–2001, Chairman, the Battery Section of the Committee of the Japanese Industrial Standard. 1996, Technical Advisor of New Material Division, Petoca, Ltd. (now Petoca Materials, Ltd.),
Awards: 1974, The Tanahashi Major Award from The Electrochemical Society of Japan. 1974, Kanto District Award from The Japanese Invention Society. 1975, The Technology Award from The Surface Technology Society of Japan. 1978, The Technology Award from The Electrochemical Society of Japan. 1978, The Minister Award from The Japan Ministry of Science and Technology. 1996, The Award of Distinguished Services from The Electrochemical Society of Japan.